GUIDANCE, NAVIGATION, AND CONTROL OF SMALL SATELLITE ATTITUDE USING MICRO-THRUSTERS

A DISSERTATION SUBMITTED TO THE GRADUATE DIVISION OF THE
UNIVERSITY OF HAWAI‘I AT MĀNOA IN PARTIAL FULFILLMENT
OF THE REQUIREMENTS FOR THE DEGREE OF

MASTER OF SCIENCE

IN

MECHANICAL ENGINEERING

DECEMBER 2016

by

Cullen Matsumoto

Dissertation Committee:

Dilmurat Azimov, Chairperson
Peter Berkelman
Reza Ghorbani

ABSTRACT

In this study, a new and automated Navigation, Guidance and Control system is designed, analyzed, simulated and tested for small satellites. As is known, this system represents the primary unit of on-board control of a flight vehicle. It consists of a set of system software algorithms and hardware elements, including various sets of sensors and electronics depending on the type of the vehicle. This study is focused on small satellites, which are becoming one of the primary tools for a wide range of low Earth and deep space missions.

The Navigation subsystem has been described in terms of its sensors and filtering technique, known as the Extended Kalman Filter. This subsystem provides the estimates of the satellite's state vector. It is assumed that this vehicle's Navigation subsystem includes GPS receiver, and accelerometer and gyro, which are considered as Inertial measurement Unit (IMU) component subsystems. The Guidance subsystem provides guidance commands for satellite's actuators, which are assumed to include a set of micro-thrusters. The Control subsystem provides control commands for increments of torque of actuation.

This study deals with the development, design and integration of the Navigation, Guidance and Control (known as GNC) subsystems into a unique framework that can be executed on-board in real time to perform satellite attitude maneuvers. The main focus is on the development of Guidance subsystem functions and algorithms. These functions, in particular, include attitude angles, angular rates and coefficients. The Guidance subsystem provides commanded angular acceleration based on a fourth-order polynomial with respect to time, which was used for lunar-descent trajectory guidance during the Moon landing maneuvers of Apollo Landers. The difference in the utility of this polynomial law in Apollo missions and this work is that in those missions this polynomial was used for trajectory guidance using numerically integrated trajectories as reference solutions. In this work, this polynomial is used to compute attitude guidance commands using a simple PD controller as an analytic reference attitude profile. The

novelty of this work is that this polynomial law is formulated and implemented for the first time for real-time and on-board attitude guidance and control using a set of microthrusters as part of the integrated GNC system. Another element of novelty is associated with targeting. A real-time targeting procedure implies on-board computations of the target states and the time remaining to achieve the target state from the current state. In this work, the target state includes Euler angles and their rates. As such, the targeting is considered as an integral and critical part of the guidance function. The guidance command is computed only after computations of the target state and is the explicit function of this state. Therefore, the proposed guidance function is considered as the ob-board target-relative attitude guidance.

The performance of the proposed GNC system has been demonstrated by two illustrative examples. In the first example, the satellite is guided to orient itself to its target position. In the second example, the satellite is guided to perform two consecutive rotational maneuvers, detumbling and reorientation, to achieve a desired attitude. The numerical simulation parameters and its results are illustrated by various plots and qualitative analysis of the relationships between the satellite's state and guidance parameters. The list of references and appendix with necessary formulas and figures are provided.

CONTENTS

LIST OF TABLES

LIST OF FIGURES

Nomenclature

α	Angular Position
$\mathbf{\Gamma}_g$	misalignment matrix
ω	Angular velocity
σ_{bi}	axial bias covariance
$\mathbf{a}_{com}$	commanded *translational* acceleration
$\mathbf{F}$	Force
$\mathbf{g}$	Gravitational acceleration
$\mathbf{p}$	Orbital position
$\mathbf{r}$	Orbital Position vector
$\mathbf{T}$	Torque
$\mathbf{v}$	Orbital velocity vector
$\mathbf{x}$	State Vector
$\mathbf{x}_c$	Current state
$\mathbf{x}_d$	Desired targeted state
Ω	Right Ascension of Ascending Node
ω	Angular Rotation rate
θ	Angular Rotation
a	acceleration
F_a	spacecraft attitude frame
F_{lo}	Spacecraft local orbital frame
F_{op}	Orbital Plane Frame
I	Inertia matrix

i	inclination angle
J	Jerk
m	Spacecraft mass
N	Perturbation forces
p_1, p_2	Arbitrary functions of time
Q	Quaternion
S	Snap
u	Control input vector
T	Time to Target
t	time

1 INTRODUCTION

The **goal** of this study is to develop, design and integrate the Navigation, Guidance and Control (GNC) functions into a unique framework that can be executed on-board of a satellite to perform attitude maneuvers using micro-thrusters. The **objectives** of this study are to 1) develop the guidance scheme using a fourth order polynomial law combined with a PD controller, 2) integrate this scheme with navigation and control functions for specific maneuvers and 3) demonstrate the execution of the resulting GNC system to perform an attitude maneuver.

The **technical approach** is the formulation of the guidance function based on the existing PD control laws and incorporate with navigation and control functions into a framework that can accept measurement data and produce guidance commands in real-time. Implementation of the proposed GNC system architectures and software algorithms are based on the functionality of this framework.

Using micro-thrusters, the small satellites and other conventional spacecraft can rapidly re-orient themselves into targeted positions or avoiding objects. This coupled with an automated GNC system can help reduce the need for human input for simple maneuvers and maintaining satellite orientation.

In this thesis, a simple GNC system for a satellite in a circular orbit is shown to orient and maintain the satellite's angular position.

1.1 Literature Review

1.1.1 Introduction

In recent years progress has been made in the development of efficient lightweight micro-thrusters. As more and more satellites orbit the earth there is a vital need to have quick responsive maneuvers to adapt to the environment. As a result, satellites need to have thrusters for rapid attitude adjustments, either for orientation of solar panels to preparing maneuvers to avoid collisions. This review is to highlight what work in the field of attitude Guidance, Navigation, and Control(GNC) of orbital satellites.

Only some elements of the current state-of-the-art GNC systems for small satellites (SS) were partially demonstrated during a few missions (PRISMA, FASTRAC, OCULUS) with two or more spacecraft using passive formation flying and attitude control [3], [4]. However, these missions do not use real-time GNC software for the attitude maneuvers. In general, the existing conventional GNC systems

- do not have explicit guidance laws implementable on ballistic or thrust trajectories,

- require iterations to achieve convergence in ground-based guidance solutions,

- utilize simplifications to control solutions leading to inaccuracies and inefficiencies in the maneuvers,

- do not have integrated real-time GNC capabilities synthesized with attitude control capabilities.

These shortcomings can be overcome by developing innovative ideas or concepts of new autonomous GNC system architectures and technologies thereby achieving maximum accuracy, efficiency and flexibility in performing the attitude maneuvers [5].

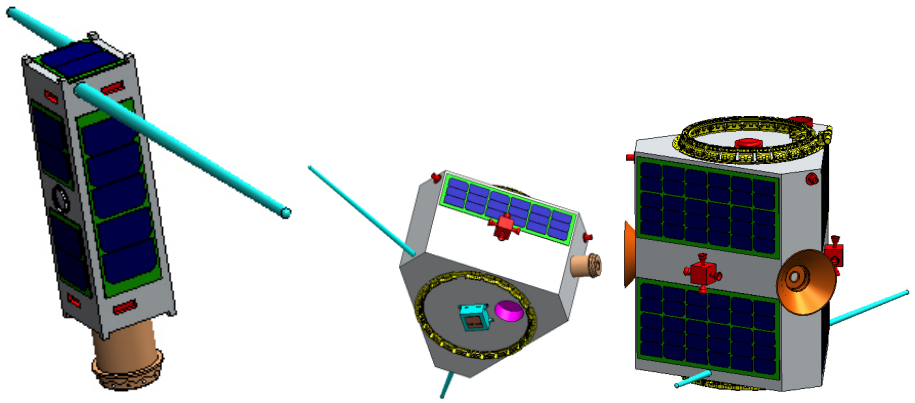

Figure 1.1: Examples of small satellites: inspector probe, science probe, conventional satellite with GNC capabilities (design).

Such technologies are classified in the NASA Draft Roadmap of Robotics, Tele-Robotics and Autonomous Systems as breakthroughs that enable new missions or potentially change missions planning with new capabilities for the next 25 years. Navigation solutions are obtained by processing lidar, inertial measurement unit (IMU) and GPS measurements in real-time. This work further advances the existing state-of-the-art on-board GNC technologies by incorporating the real-time GNC functionality [6]. This functionality is known to be critical in performing the attitude maneuvers and can be enabled only by utilizing optimal, explicit and closed-form attitude control solutions integrated with the relative- motion solutions (see Fig.1.2).

Recent advances in SS technology, as well as the new requirements for one or more spacecraft systems and their operational responsiveness, suggest that new and innovative approaches to develop and implement on-board software for controlling and guiding spacecraft utilizing navigation solutions are needed. These requirements, such as enabling spacecraft to access a wider range of altitudes, orbital inclinations and attitudes, and performing various CPO autonomously and efficiently necessitate innovative approaches to and concepts for the architecture, configuration and functionality of the spacecraft GNC system.

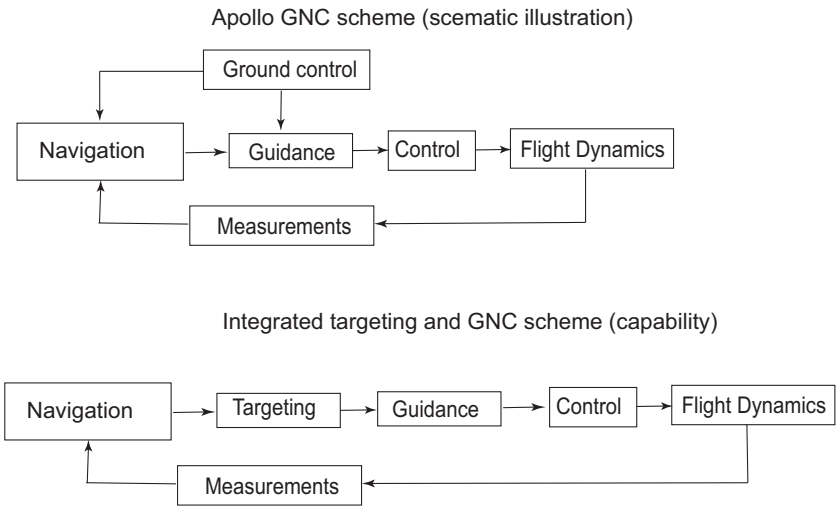

Figure 1.2: Functional diagrams of conventional GNC and proposed TGNC

Definitions

(SS) is defined as ESPA class (180kg) or less. Where proposers target a specific class of small spacecraft, the following wet mass range definitions apply:

Minisatellite, 100 kilograms or higher

Microsatellite, 10-100 kilograms

Nanosatellite, 1-10 kilograms

Picosatellite, 0.01-1 kilograms

Femtosatellite, 0.001-0.01 kilograms.

1.1.2 Control

A good deal of papers that are currently available on the Subject of Attitude Control are generally very focused. For the most part these papers will focus on control methods or navigation filters. They often have either an assumption that the sensors are perfect, or use an estimation tool such as an Extended Kalman Filter to estimate the satellite's position and orientation [7, 8]. In general, the sources of torque in these studies were varied from reactions wheels to magnetic torque rods, along with an occasional mini-thruster. There is a limited quantity of papers on attitude control using micro-thrusters. In Souza's paper, the analysis of a State Dependent Riccati Euation was compared with a Linear Quadratic Regulator for the use of a control system [9]. This was in conjunction with a Kalman Filter and found that that Riccatri controller was superior to the Linear Quadratic Regulator. However there was no comparisons to a state feedback control system in the paper. Min's paper on the other hand used a state feedback controller [10]. This paper however did show that the controller needs to be calibrated to avoid

overshooting its goal and settling in a cycle. In the study for the FalconSat-3 the PD controller using the state feedback was able to reach the desired orientation[7].

PID controllers were described with details in Ref [11, 12, 13, 14, 15, 16]. These controllers have become very useful and effective controllers used in a wide range of controllable systems, including spacecraft, mussels, unmanned aerial systems, and submarines. Their success relies on the flexibility of choosing the coefficients, which allows us to satisfy various terminal conditions and requirements [13]-[16].

Classical linear controller is another well known and widely used classical controller, which is expressed as $u = -Kx$, where K is the controller gain, and $\mathbf{x}$ is the state vector [11],[12]. Both of these controllers have been shown to be useful and efficient for real-time applications.

Analysis of H-infinity controllers have been provided in [17]. These types of controllers have been shown useful in some systems, but their utility is associated with lengthy analysis, and this feature negatively impacts on their applicability for on-board systems.

Other modern studies of problems with nonlinear control are provided in Ref. [18], which is the collection of various papers devoted to control analysis. Some of the papers deal with the utility of the canonical equations for modern nonlinear control problems, which have been shown integrable with mainly numerical methods [16],[18]. The area of optimal control problems is another important area related to GNC system implementation. Such problems represent topics of the future studies, and are not considered in this work [11],[16].

Modeling

For the kinematic models the Euler angles are used as a basis as seen in many different papers [19, 20, 21, 22]. However this can be then converted into a quaternion if need be [20]. At the same time the body of the satellite can be modeled as a rigid body, which is the most common for smaller satellites, or a flexible body if it includes solar panel booms [21].

In addition there are many other various methods to represent attitude as seen in Shuster's survey [23]. In addition to quaternion and Euler angles, Shuster also goes over Transformation matrices, and many variations such as the Euler-Rodrigues parameters.

Control Schemes

In terms of control of satellites there are many different methods. In general thrusters are controlled to be on or off. The main difference is the method of control. Pulse-Width Pulse-Frequency Modulation can be used to control the length of the duration the thruster is active [24, 10].

There are other methods of modulation mentioned by Lee such as the Bang-Bang control system, as well as the bang-off-bang system [24]. Also mentioned is the input shaping

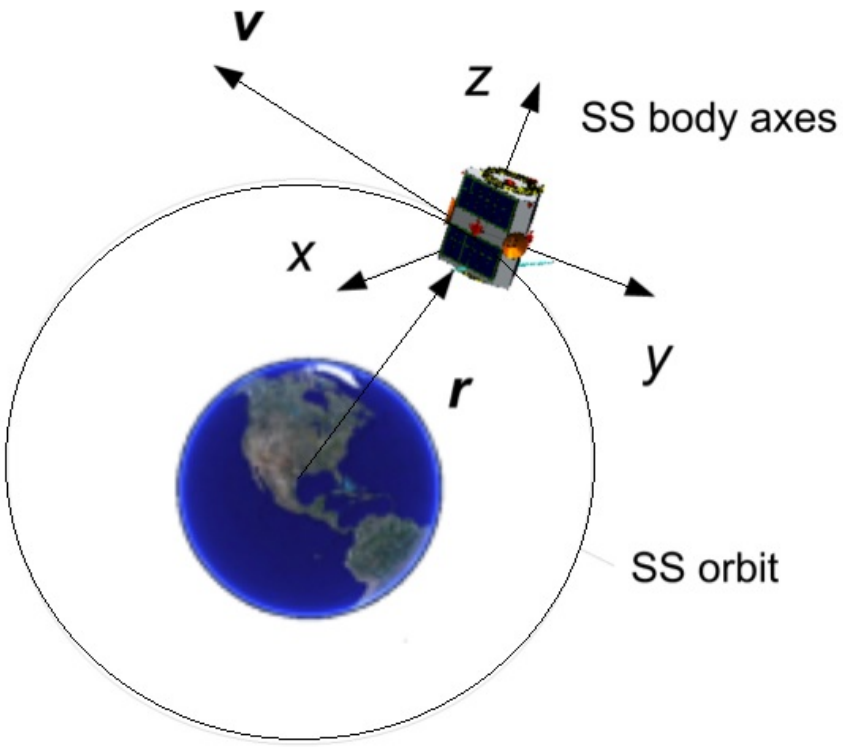

Figure 1.3: Small satellite orbit and associated body coordinate system

techniques using impulses and the pulse width modulation (PWM). It is here that the limitations of some of these control schemes are stated, such as the ”excessive thruster action” via the bang-bang controller [24].

It is mentioned that the PWPF and the PWM are fundamentally the same, as they are both based around the Schmidt trigger [24]. The only difference is that the pulse duration is modified in the PWPF while the PWM stays the same.

Control actuators: Thrusters

Thrusters have come a long way from the days of the Apollo Mission. Research is being done constantly in improving the fuel efficiency of these thrusters, while at the same time reducing the sizes for usage in smaller satellites. With the propagation of small satellites, there lies a need for capabilities in maneuvering that are similar to larger satellites [25].

For example in Florin Mingireanu’s paper shows the potential of using a hybrid thruster [26]. In the paper, the hybrid rockets are proposed to be safer and simpler then liquid based rockets, while at the same time having improved reaction times. It was also mentioned how the actual force created by the thruster can be controlled via the mass flow rate of the oxidizer [26].

If however thrust can be in the micro-newton range then Field-Emission Electric Propulsion (FEEP) can be used [27]. In Marcuccio’s paper it is mentioned how 16 thrusters can

be used to control attitude without any usage of reaction wheels, while at the same time have the flexibility to do some translational maneuvers. It is noted that FEEP thrusters are only viable in certain environments as they provide low thrust.

Additional Micro-Thrusters include Ion Electrospray Propulsion Systems for Cubesats [28]. This system provides a thrust in the 100 μN range. Another system made specifically for Cubesats is the Vaccum Arc Thruster which has a thrust of 54 μN. This thruster is being researched by the University of Illinois and is planned to be placed upon their satellite [29].

1.1.3 Navigation

Within the GNC system there lies a need for knowing the state of the satellite. Knowing or at least estimating the current angular position, velocity, and acceleration allows for the guidance system to make the necessary commands to bring the satellite to its targeted state.

Attitude Representation

There are many different ways for representing attitude for calculations. Most common are Euler angles and Quaternions [30]. Euler angles are often used for its simplicity and ease of use, however they can give rise to singularities. On the other hand Quaternions do not have this problem. As a result Quaternions are widely used in many different missions including the European Space Agency's (ESA) Student Space Exploration and Technology Initiative (SSETI) [31]. It should be noted that there are other methods of representing attitude, each with their own advantages and disadvantages such as the Rodrigues parameters.

Sensors

In Kaplan's book there are many different types of sensors used to determine a satellites current attitude [32]. Although dated, it mentions many different methods that are still in use today. This includes sun sensors that determine orientation based upon the light of the sun hitting sensors located behind a slit. Again Kalpan mentions that there are two classifications of sun sensors, Digital and Analog.

At the same time when the satellite is unable to sense the sun, star sensors can be used. Depending on the orbit the star it uses can change. Either Canopus or Polaris are used due to their location and brightness [32]. Also mentioned are Earth sensors that use the horizon to determine the attitude of the satellite.

In more recent times other methods of navigation have been developed. For example the Trailblazer satellite uses the Global Positioning System (GPS), Inertial Measurement Units (IMU), and magnetometers to help determine its position and attitude [33, 34].

Kalman Filters

One of the first things that was mentioned in many papers was the usage of filters for estimations. This was primarily to estimate the state of the satellite in the next time step. However, one of the most crippling aspects of the Kalman Filter is the fact that is requires the equations to linearized in order to be used.ized in order to be used. In Souza's paper, the usage of the Kalman Filter allows for better performance in obtaining the desired attitude state[35, 9].

Using the Extended Kalman Filter (EKF) allows for non-linear equations to be used, as opposed to linearizing the equations. This can be useful for many applications. Primarily due to the fact that linearizing equations simplifies dynamical equations and reduces the dynamical model's capability to calculate many additional factors.

1.1.4 Guidance

Guidance in general is the ability of the system to determine its actions to reach its goal. As a result it requires inputs that determine current position and velocity. In the case of attitude control the angular position of the satellite as well as the readings from the IMUs are important for the guidance algorithm to determine the input to the control system. It is mentioned that missions are often dependent on the guidance algorithm's to stay on target, or avoid damaging sensors via the sun [33]. By having an appropriately planned guidance algorithm it is possible to reduce the cost and increase the success rate of missions in space. The paper in particular focuses on the avoidance of certain orientations that would endanger the satellite's equipment due to it's sensitivity to the sun's rays. It further goes into detail in regards to the logic behind the algorithm to provide the most time on target, while at the same time avoiding the exclusion zone. It is via Guidance that the satellite knows the next step that needs to be taken to reach its objective.

Guidance laws. The *original and general concept of guidance*, obtained first by George Cherry, a MIT staff member, and known as the explicit (E)-guidance, is given by formula:

$$\mathbf{a}_{com} = \mathbf{c}_1(\mathbf{x}_c, \mathbf{x}_d)p_1(t) + \mathbf{c}_2(\mathbf{x}_c, \mathbf{x}_d)p_2(t) - \mathbf{g}$$

where $\mathbf{a}_{com}$ is the commanded *translational* acceleration, $\mathbf{x}_c$ and $\mathbf{x}_d$ are the current ("c") and desired ("d") (target) states, and $\mathbf{g}$ is the gravitational acceleration, and p_1 and p_2 are arbitrary functions of time [36]. Alan Klumpp, an Apollo engineer, adjusted this formula to obtain his quartic polynomial- based lunar descent guidance formula, which then was implemented in all Apollo missions: a thrust acceleration to be commanded at any point in space consists of three terms: the acceleration of the reference trajectory at a particular time, minus two feedback terms proportional to velocity and position deviations from the reference trajectory [37]. Furthermore, various guidance laws or schemes have been developed regardless of the control actuation devices

as a continuation of an optimal control problem, and by employing the quartic polynomial, Lyapunov's second method, the $\mathbf{v}$-nulling method, the vision-based guidance and other numerical, approximate and analytical methods [38]-[39].

In most cases, these guidance schemes rely on approximate or numerical trajectory and control solutions, they are not formulated for an autonomous implementation, and the guidance targets are considered as predetermined inputs [40]-[41]. For example, the Lunar landers of all Apollo missions used precomputed target states, the existing "Orbital Express" spacecraft or Mars "Curiosity" lander's guidance schemes were designed for the low- and high-thrust respectively using highly approximate and iterative control algorithms [42]-[43]. In addition, the recent small satellite missions, such as FASTRAC, OCULUS and PRISMA aimed to demonstrate on-board estimation or precomputed control capabilities (Fig.5.1) [44]. Note also that no autonomous and integrated trajectory and attitude dynamics, estimation and guidance have been reported to date.

1.1.5 Guidance, Navigation, and Control for attitude

In general there is a lack of GNC packages for attitude controls. As seen previously all research has been focused in specific areas of GNC such as the control systems. As a result there is very little research done in this particular field and limits the capability of satellites to be autonomous. Currently there have been many studies using Navigation and Control together to create an autonomous or near autonomous systems. Examples include the Prox-1 which was a full package for automating a specific set of maneuvers after deployment [45]. Another example of work towards a complete GNC of attitude is the CanX-4/5 which uses attitude control to orient itself for usage of its only thruster [46].

At the same time there are studies that focuses more so on attitude control, however they do not include Guidance within the loop, thus relying primarily on the Control subsystem. Examples include a study on control algorithms for the FalconSat-3 [7]. It should be noted that that relied upon an assumption that the sensor was perfect. Again for various CanX satellites, a study was made using a loop with and Extended Kalman Filter and a Controller [8].

FASTRAC

FASTRAC is a mission sent up in November 2010 where two satellites are to perform maneuvers relative to one another using on-board sensors 5.1. The results are then compared to ground-side calculations [44]. The data used for navigation was from the GPS sensors. This then was used for controlling the thrusters to allow for attitude orientation [44].

PRISMA

PRISMA is a project by the Swedish National Space Board, dedicated to formation flying and rendezvous. The satellites are meant to have autonomous capabilities for formation

flying, along with rendezvous capabilities[44]. The PRISMA mission has been successful in its demonstration of autonomous formation flying, along with rendezvous.

OCULUS

OCULUS is a program designed for to help aid the United States Space Situation Awareness by providing a satellite that is capable of capturing images and being used as a telescope calibration object. It will be able to track and capture images of cube-sats using imagining sensors[44].

OREOS

OREOS was a mission launched by NASA with the intent to demonstrate the capabilities of cubesats for the purpose of data collection with autonomous nano-satellites. This mission was used to prove the capabilities of off the shelf materials for nano-satellites to show that carrying and conduction experiments can be done with cheaper satellites [44].

1.2 Concluding remarks

The review of the literature has revealed the following aspects of existing studies of the SS technologies:

Propulsion, Communications, Prox Ops and other SS technologies of interest. The studies of the existing work in all these areas converge to some set of problems that can be addressed in the context of a dedicated mission (such as FASTRAC, OCULUS, OREOS, PRISMA). The current needs for research and technology development in each of these areas can be reduced to the following issues of interest:

1. Development of solutions and corresponding algorithms for – orbit determination and attitude control using measurements (IMU, rang, range-rate, star-camera, etc.); – controlled and forced relative motion; – formation flying.

2. Guidance and control algorithms for propulsion system (electrical or chemical propulsion developed for SS). Only Orbital Express mission has demonstrated low-thrust trajectory guidance (but it was not a small sat).

3. Development and tests of autonomous, on-board, real-time GNC software for selected attitude maneuver scenarios are of critical interest.

2 SATELLITE MODEL

A 1U CubeSat has a dimension of 10 cm x 10 cm x 10 cm and a mass of 1 kg. This is the basis of dynamic model of the satellite in addition to the moments of inertia.

2.1 Satellite Coordinate System/Reference Frames

For satellites coordinate frames need to be defined to determine how they are referenced in relation to either the motion or towards other objects. Orbital reference frames are used to to describe the motion of a spacecraft within an orbit. They are the orientation of the orbit in relation of the inertial space of the spacecraft and in relation to the Earth.

On the other hand spacecraft can also have a local orbital reference frame. This framework would be in relation to specific points or in relation to other orbital objects. And finally there is the spacecraft attitude and body frame which is in relation to the center of mass of the spacecraft.

Earth Centered Intertial system: originates from the Earth center of mass, the Z axis points through the geographic North Pole, or the axis of rotation. The X axis is in the direction of the vernal equinox, and the Y axis completes the right-handed triad.

Body coordinate system: originates from the satellites mass center. This frame is fixed in the body. The X-axis and Z-axis are such that moments of inertia matrix is diagonal, and the Y-axis completes the right handed triad.

The Local Vertical Local Horizontal system: originates from the satellites center of mass, the Z-axis is directed towards the Earth center of mass, Y-axis is directed towards the opposite to the normal to the orbital plane, and the X-axis completes the triad.

All three coordiante frames can be seen in Figure 2.1.

2.1.1 Orbital plane frame

The orbital plane frame F_{op} is used for the motion of the orbital plane is described. As seen in Figure 2.1 the orbital plane frame is similar to the Earth centered equatorial frame, however it is not limited to a set orientation.

As seen in Figure 2.1 the axis z is in the orbital plane, however it is pointed towards the ascending node, while the axis y is normal to the orbital plane while pointed in the northern direction. Axis x is orthogonal to z and y on the orbital plane. Since the coordinate frames are similar, just rotated, the Earth centered equatorial frame can be transformed into the the orbital plane frame using the equation below.

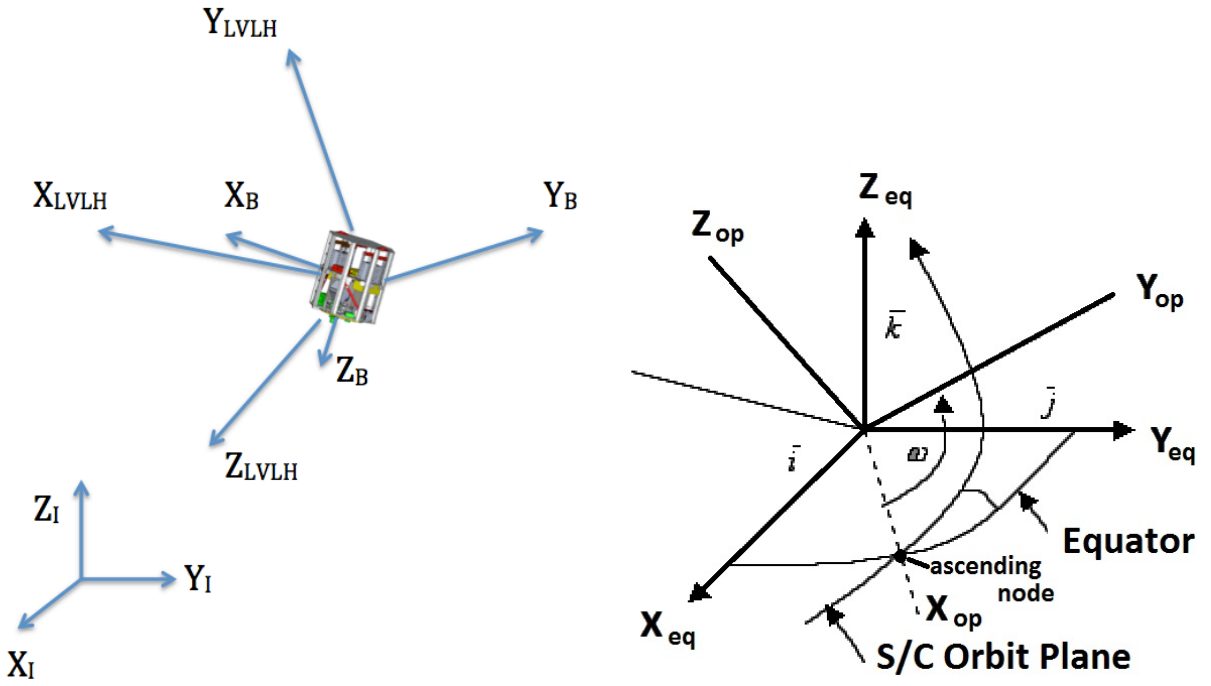

Figure 2.1: Earth Centered Inertial, body and LVLH coordinate systems on the left. Also shown is the Orbital plane frame on the right [1]

$$\begin{bmatrix} x_{op} \\ y_{op} \\ z_{op} \end{bmatrix} = \begin{bmatrix} 1 & 0 & 0 \\ 0 & \cos(i) & \sin(i) \\ 0 & -\sin(i) & \cos(i) \end{bmatrix} \begin{bmatrix} \cos(\Omega) & \sin(\Omega) & 0 \\ -\sin(\Omega) & \cos(\Omega) & 0 \\ 0 & 0 & 1 \end{bmatrix} \begin{bmatrix} x_{eq} \\ y_{eq} \\ z_{eq} \end{bmatrix} \tag{2.1}$$

Where i is equal to the inclination angle. and Ω is the Right Ascension of Ascending Node(RAAN). The RAAN is the angle from the point of the vernal equinox and the ascending node. The orbital plane vectors for the axis is the $x_{op}, y_{op}, and z_{op}$ and the $x_{eq}, y_{eq}, and z_{eq}$ is the axis vectors for the Earth centered equatorial frame.

2.1.2 Spacecraft local orbital frame

Spacecraft local orbital frame is referred as F_{lo} is used to describe motions in reference to the center of the Earth. This is used for orbiting bodies and has one of the axis's pointed to the center of the Earth at all times. As seen in Figure 2.2 [32].

The origin of the coordinate system is the center of mass of the spacecraft. The axis x is the direction of the orbital velocity. Axis y is the is perpendicular to the plane that the orbit is upon and z is pointed directly to the center of the Earth at all times.

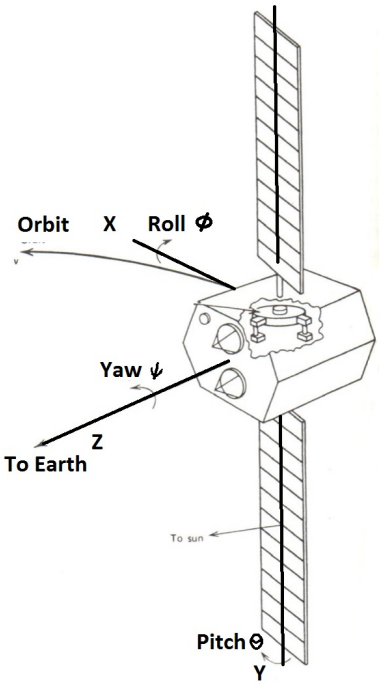

Figure 2.2: The Spacecraft local orbital frame

2.1.3 Spacecraft attitude frame

The spacecraft attitude frame (F_a) is used to describe the rotations of the satellite. As opposed to the Local orbital frame the axis of the is not fixed to certain orientations, instead is dependant on the mission parameters and phase of the mission. Due to changes in the center of mass of the satellite this can change during the mission.

In the figure above the origin of the frame is at the center of mass, while the axis form a right handed system. This framework can be converted to the local orbital frame using the equation below.

$$\begin{bmatrix} x_a \\ y_a \\ z_a \end{bmatrix} = \begin{bmatrix} 1 & 0 & 0 \\ 0 & c\alpha_x & s\alpha_x \\ 0 & -s\alpha_x & c\alpha_x \end{bmatrix} \begin{bmatrix} -s\alpha_y & 0 & c\alpha_y \\ 0 & 1 & 0 \\ c\alpha_y & 0 & s\alpha_y \end{bmatrix} \begin{bmatrix} c\alpha_z & s\alpha_z & 0 \\ -s\alpha_z & c\alpha_z & 0 \\ 0 & 0 & 1 \end{bmatrix} \begin{bmatrix} x_{lo} \\ y_{lo} \\ z_{alo} \end{bmatrix} \tag{2.2}$$

where the attitude angles are α_z (azimuth), α_y (elevation), and α_x (roll). Note that s and c are short for $\sin$ and $\cos$. This results in the vectors $x_a, y_a, and z_a$ which are the frame vectors for the spacecraft attitude frame (F_a).

2.2 Representation of Attitude

2.2.1 Euler Angles

Euler angles are based upon the concept of any orientation can be represented by a series of three consecutive rotations [23]. However Euler angles do have issues with a phenomenon called the gimbal lock where upon certain conditions the Euler angles simply zero out[23].

Below are the three single axis rotation matrices with θ_1, θ_2, and θ_3 are ψ, θ, and ϕ respectively.

$$[M(\theta_1)] = \begin{bmatrix} 1 & 0 & 0 \\ 0 & \cos\theta_1 & \sin\theta_1 \\ 0 & -\sin\theta_1 & \cos\theta_1 \end{bmatrix} \tag{2.3}$$

$$[M(\theta_2)] = h \begin{bmatrix} \cos\theta_2 & 0 & -\sin\theta_2 \\ 0 & 1 & 0 \\ \sin\theta_2 & 0 & \cos\theta_2 \end{bmatrix} \tag{2.4}$$

$$[M(\theta_3)] = \begin{bmatrix} \cos\theta_3 & \sin\theta_3 & 0 \\ -\sin\theta_3 & \cos\theta_3 & 0 \\ 0 & 0 & 1 \end{bmatrix} \tag{2.5}$$

with $(\theta_1, \theta_1, \theta_1) = (\psi, \theta, \phi)$ respectively. If using the rotation matrix with the order of ψ, θ, and ϕ the direction cosine matrix $[C]$ is:

$$[C] = \begin{bmatrix} c\theta_2 c\theta_1 & c\theta_2 s\theta_1 & -s\theta_2 \\ s\theta_3 s\theta_2 c\theta_1 - c\theta_3 s\theta_1 & s\theta_3 s\theta_2 s\theta_1 + c\theta_3 c\theta_1 & s\theta_3 c\theta_2 \\ c\theta_3 s\theta_2 c\theta_1 + s\theta_3 s\theta_1 & c\theta_3 s\theta_2 s\theta_1 - s\theta_3 c\theta_1 & c\theta_3 c\theta_2 \end{bmatrix} \tag{2.6}$$

where (θ_1, θ_2, θ_3) = (ψ, θ, ϕ) respectively.

in terms of angular rotation rate $(\omega_x, \omega_y, \omega_z)$ the Euler angle for a 3-2-1 rotation (ψ, θ, and ϕ rotation order) can be expressed as:

$$\begin{bmatrix} \omega_x \\ \omega_y \\ \omega_z \end{bmatrix} = \begin{bmatrix} -\sin\theta & 0 & 1 \\ \sin\phi\cos\theta & \cos\phi & 0 \\ \cos\phi\cos\theta & -\sin\phi & 0 \end{bmatrix} \begin{bmatrix} \dot{\psi} \\ \dot{\theta} \\ \dot{\phi} \end{bmatrix} \tag{2.7}$$

However even with all the issues with Euler angles they were used in this simulation due to the ease and simplicity of implementing them into the code. At the same time the issue of

gimbal locks are worked around by keeping the maneuvers small, thus preventing the chances of the satellite meeting the requirements of encountering it.

2.2.2 Quaternions

A quaternion is a four parameter system which uses 3 vectors and a rotation about an axis. The rotation is directed around an axis as defined by the 3 vectors a_1, a_2, and a_3. The basic quaternion equation can be seen below [23, 8, 47].

$$\mathbf{Q} = \begin{bmatrix} q_1 \\ q_2 \\ q_3 \\ q_4 \end{bmatrix} = \begin{bmatrix} a_1 \sin(\frac{\phi}{2}) \\ a_2 \sin(\frac{\phi}{2}) \\ a_3 \sin(\frac{\phi}{2}) \\ \cos(\frac{\phi}{2}) \end{bmatrix} = \begin{bmatrix} \mathbf{q} \\ q_4 \end{bmatrix} = \begin{bmatrix} \mathbf{a} \sin(\frac{\phi}{2}) \\ \cos(\frac{\phi}{2}) \end{bmatrix} \tag{2.8}$$

The quaternion has a unique relation with each of its component parts, where the sum of the squares is equal to one.

$$q_1^2 + q_2^2 + q_3^2 + q_4^2 = 1 \tag{2.9}$$

The quaternion can be found by using the Direction Cosine Matrix (DCM) as seen in the equations below.

$$\mathbf{a} = \begin{bmatrix} a_1 \\ a_2 \\ a_3 \end{bmatrix} = \frac{1}{2\sin(\phi)} \begin{bmatrix} C_{23} - C_{32} \\ C_{31} - C_{13} \\ C_{12} - C_{21} \end{bmatrix} \tag{2.10}$$

where $C_{ij}, i, j = 1, 2, 3$ are the elements of DCM. . This equation can be eventually be reduced down to:

$$\begin{aligned} q_1 &= \frac{1}{2s}(C_{23} - C_{32}) \\ q_2 &= \frac{1}{2s}(C_{31} - C_{13}) \\ q_3 &= \frac{1}{2s}(C_{21} - C_{12}) \\ q_4 &= \frac{s}{2} \end{aligned}$$

to find individual parts of the Quaternion using the DCM.

2.3 Problem Statement

Consider a spacecraft moving with a limited power and limited specific impulse in a central Newtonian gravity field. Let $\mathbf{r}$ and $\mathbf{v}$ be the position and velocity vectors of the

spacecraft's center of mass, and let m be the spacecraft's mass. The vector functions $\mathbf{r}$ and $\mathbf{v}$, and the scalar function m are considered to be continuous, but their time derivatives may have discontinuities of the first order. The spacecraft is powered by a propulsion system with thrust $\mathbf{F}$ to control the translational motion, exhaust power P and specific impulse I_{sp}, and with a reaction control system (RCS) thrust vector, $\mathbf{T}$ to control the attitude. If the vector functions $\mathbf{x} = [\mathbf{r}, \mathbf{v}, m, \mathbf{q}, \boldsymbol{\omega}]^T$ denotes the state vector, then the equations of motion of the spacecraft can be given as: [48]

$$\dot{\mathbf{x}} = \mathbf{f}(\mathbf{x}, \mathbf{u}) \tag{2.11}$$

with

$$\mathbf{x} = \begin{bmatrix} \mathbf{r} \\ \mathbf{v} \\ m \\ \mathbf{q} \\ \boldsymbol{\omega} \end{bmatrix}, \quad \mathbf{f}(\mathbf{x}, \mathbf{u}) = \begin{bmatrix} \mathbf{v} \\ -\frac{\partial U}{\partial \mathbf{r}} + \mathbf{a}_{all} \\ -\frac{||\mathbf{F}||}{I_{sp} g_0} \\ \frac{1}{2}\mathbf{B}(\boldsymbol{\omega})\mathbf{q} \\ \mathbf{I}^{-1}\left[-\boldsymbol{\omega} \times \mathbf{I}\boldsymbol{\omega} + \mathbf{N} + \mathbf{T}\right] \end{bmatrix}, \quad \mathbf{u} = \begin{bmatrix} \mathbf{F} \\ I_{sp} \\ \mathbf{T} \end{bmatrix},$$

where

$$\mathbf{a}_{all} = \mathbf{a}_{aero} + \mathbf{a}_{solar} + \mathbf{a}_{thrust} + \mathbf{a}_{rel-eff} + \mathbf{a}_{multi-body} + \mathbf{a}_{other},$$

and $\mathbf{r}$ is the satellite position vector originated from COM of attracting planet,

$\mathbf{a}_{nonsp}$ is the acceleration due to non-spherical planet gravitation,

$\mathbf{a}_{aero}$ is the acceleration due to aerodynamics forces,

$\mathbf{a}_{multi-body}$ is the acceleration due to multi-body effects (from Sun, Moon, ...),

$\mathbf{a}_{solar}$ is the acceleration due to solar radiation pressure,

$\mathbf{a}_{thrust}$ is the acceleration due to propulsive thrust,

$\mathbf{a}_{rel-eff}$ is the acceleration due to relativistic effects,

$\mathbf{a}_{other}$ is the acceleration due to other effects, such as magnetic fields, solid-Earth tides, ocean tides, the function U is the Earth's potential function, gravitational parameter of the central body, and g is the sea-level gravitational acceleration, $\mathbf{I}$ is the inertia matrix, $\mathbf{q}$ is the quaternion consisting of quaternion vector $(q_1,\ q_2,\ q_3)$ and scalar, q_4, and $\mathbf{u}$ is the control input vector, $\mathbf{F}$ and $\mathbf{T}$ are the thrust control and torque control vectors, $\mathbf{N}$ is the torque of the perturbation forces.

It should be noted that the translational motion of the satellite can be reduced into easy to derive equations. This is the result of the satellite being in a geo-stationary circular orbit which reduces the acceleration acting upon the satellite to just gravity. This allows for the translational motion to be simplified to allow for more emphasis on the attitude motion. However since this is still a rigid body system they both will continue to impact each other, abet in a minor function. This is opposed to other studies where translational and attitude motions are dealt with separately [49, 2].

$\mathbf{F}$ and $\mathbf{T}$ are subject to the constraints:

$$0 \leq ||\mathbf{F}|| \leq ||\mathbf{F}||_{max}, \quad 0 \leq ||\mathbf{T}|| \leq ||\mathbf{T}||_{max}, \qquad I_{sp_{min}} \leq I_{sp} \leq I_{sp_{max}}, \tag{2.12}$$

where $||\mathbf{F}||_{max}$ and $||\mathbf{T}||_{max}$ are given maximum allowable values of $\mathbf{F}$ and $\mathbf{T}$, and $I_{sp_{min}}$ and $I_{sp_{max}}$ are the given minimum and maximum specific impulse. The functions Ψ_l $(l = 1, ..., q_1)$ and F_k $(k = 1, ..., q_2)$ are assumed to be continuous and possess continuous partial derivatives of sufficiently high order on all their arguments.

The objective is to transfer the spacecraft from the initial configuration given by

$$\Psi_l(x_{01}, x_{02}, ..., x_{0n}, t_0) = 0, \qquad l = 1, ..., q_1, \quad q_1 \leq n + 1 \tag{2.13}$$

at time instant t_0 to the final configuration given by

$$F_k(x_{11}, x_{12}, ..., x_{1n}, t_1) = 0, \qquad k = 1, ..., q_2, \quad q_2 < n + 1 \tag{2.14}$$

at time instant t_1 while remaining directly above or repeatedly flying over a specified Earth target at a desired altitude with a desired attitude configuration[48].

As seen in Figure 2.3, the Cartesian coordinates and rates can be connected to classical orbital elements via the relationships between standard Cartesian Coordinates and Spherical Coordinate systems. In Vallado's book the orbital elements can be used to find orbital position and velocity ($\mathbf{r}$ and $\mathbf{v}$). This can also be reversed to find the six classical orbital parameters (Keplerian)[2].

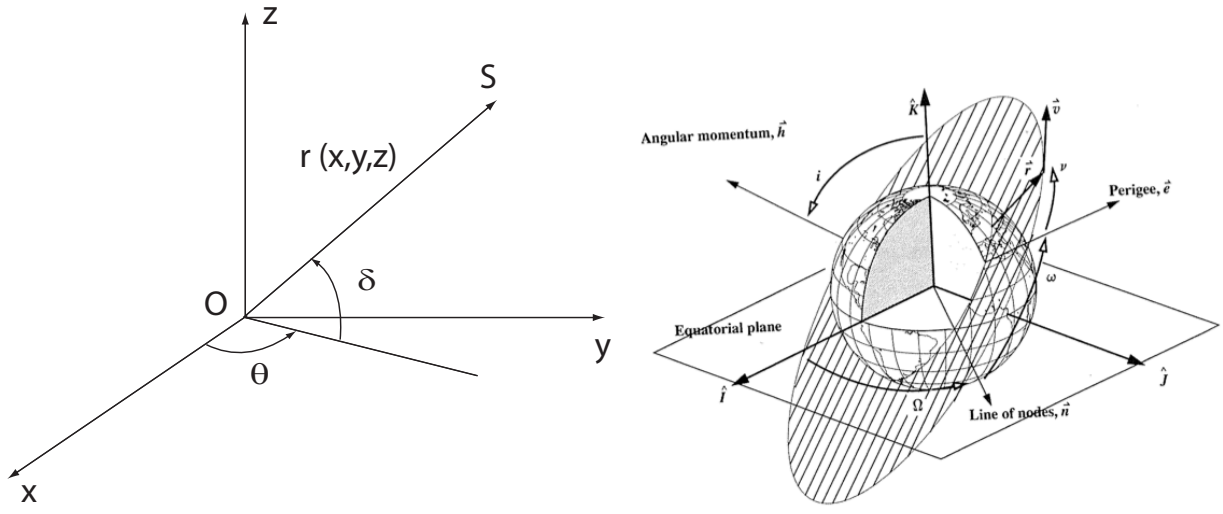

Figure 2.3: Spherical coordinate system and the Classical Orbital Elements [2].

2.4 Equations of Attitude Motion

The state vector of the of the satellite is comprised of a vector component. First is the orbital elements of $\mathbf{p}$ and $\mathbf{v}$ which represent the orbital position and velocity of the satellite respectively. After that is the attitude angle α and attitude angular rate ω. The angular rate is in respect to the spacecraft body frame, thus if needed must be adjusted if need be. Below is the equations representing the state vector of the satellite.

$$\mathbf{x} = [p, v, \alpha, \omega]^T \tag{2.15}$$

with

$$\mathbf{p} = \begin{bmatrix} x \\ y \\ z \end{bmatrix} \tag{2.16}$$

$$\mathbf{v} = \begin{bmatrix} \dot{x} \\ \dot{y} \\ \dot{z} \end{bmatrix} \tag{2.17}$$

$$\boldsymbol{\alpha} = \begin{bmatrix} \psi \\ \theta \\ \phi \end{bmatrix} \tag{2.18}$$

$$\boldsymbol{\omega} = \begin{bmatrix} \omega_x \\ \omega_y \\ \omega_z \end{bmatrix} \tag{2.19}$$

In order to determine the angular position and rate of the satellite, the dynamical model must be generated via the Equations of motion. The basic component equations used come from Kaplan's book as seen in the equations below[32].

$$T_x = I_x\, \dot{\omega_x} + \omega_y \omega_z (I_z - I_y), \tag{2.20a}$$

$$T_y = I_y\, \dot{\omega_y} + \omega_x \omega_z (I_x - I_z), \tag{2.20b}$$

$$T_z = I_z\, \dot{\omega_z} + \omega_x \omega_y (I_y - I_x) \tag{2.20c}$$

Where T_i is the torque from the micro-thrusters around the i axis with $i = (x, y, z)$. I_i is the moment of inertia around the i axis with $i = (x, y, z)$. Note that the diagonals of the moment of inertia are the only moments used for the purpose of this simulation[32].

From here the equations are further refined to take into account the coordinate system and how the orbit of the satellite affects the angular position. In such a case the equations from Kaplan's book are shown below[32].

$$T_x = I_x\ \ddot{\phi} + a\phi + b\dot{\psi}, \tag{2.21a}$$

$$T_y = I_y\ \ddot{\theta} + e\theta, \tag{2.21b}$$

$$T_z = I_z\ \ddot{\psi} + c\psi - b\dot{\phi} \tag{2.21c}$$

$$a = 4\omega_o^2(I_y - I_z), \tag{2.22a}$$

$$b = -\omega_o(I_x - I_y + I_z), \tag{2.22b}$$

$$c = \omega_o^2(I_y - I_z), \tag{2.22c}$$

$$e = 3\omega_o(I_x - I_z) \tag{2.22d}$$

given that $I_x = I_z$, $e = 0$. This allows the equations to be reduced to:

$$T_x = I_x\ \ddot{\phi} + a\phi + b\dot{\psi}, \tag{2.23a}$$

$$T_y = I_y\ \ddot{\theta}, \tag{2.23b}$$

$$T_z = I_z\ \ddot{\psi} + c\psi - b\dot{\phi} \tag{2.23c}$$

The purpose of these equations is to allow the coordinate frame to continue pointing towards the center of the Earth while staying in orbit. The ω_o is the rotation due the orbital motion of the spacecraft.

In this work only Newtonian gravitational acceleration is considered, $\mathbf{F}$ and Isp are assumed constant, Ψ_k represents the initial position of the satellite in orbit, and F_k represents its final position in orbit.

$$\dot{x} = v_x, \tag{2.24}$$
$$\dot{y} = v_y, \tag{2.25}$$
$$\dot{z} = v_z, \tag{2.26}$$
$$\dot{v_x} = -\frac{\mu}{r^3}x, \tag{2.27}$$
$$\dot{v_y} = -\frac{\mu}{r^3}y, \tag{2.28}$$
$$\dot{v_z} = -\frac{\mu}{r^3}z, \tag{2.29}$$
$$\dot{\phi} = \dot{\phi}_o + \dot{\omega_x} * dt, \tag{2.30}$$
$$\dot{\theta} = \dot{\theta}_o + \dot{\omega_y} * dt, \tag{2.31}$$
$$\dot{\psi} = \dot{\psi}_o + \dot{\omega_z} * dt, \tag{2.32}$$
$$\dot{\omega_x} = \frac{T_x - (a\phi + b\dot{\psi})}{I_x}, \tag{2.33}$$
$$\dot{\omega_y} = \frac{T_y}{I_y}, \tag{2.34}$$
$$\dot{\omega_z} = \frac{T_z - (c\psi + b\dot{\phi})}{I_z}, \tag{2.35}$$

From this point the angular acceleration of the satellite was obtained and the equations of angular motion was generated. It should be noted that it is assumed that the angular changes will be under $+/-$ 10 degrees at most. As a result it is possible to work in Euler angles as opposed to using quaternions.

2.5 Thruster Configurations/Specifications

The Micro-Thrusters available for CubeSat attitude control is limited. Currently MIT has research ongoing on a ion Electrospray Propulsion System for Cubesats[28]. With the current published papers the thrust generated by this system is in the 100 μN range [50]. Though this is greater then some of the current micro-thrusters in used for attitude control as seen in a satellite to be launched by the University of Illinois that uses a Vacuum Arc Thruster with a thrust of 54 μN [29].

In general for attitude control 12 thrusters are used. This can be seen in Figure 2.5. The thrusters are paired together to generate the moment for attitude corrections. At the same time due to the thrusters working in tandem, the trajectory of the satellite would not be affected. As seen below in Figure the positions of the thrusters are distributed on the satellite evenly. For the

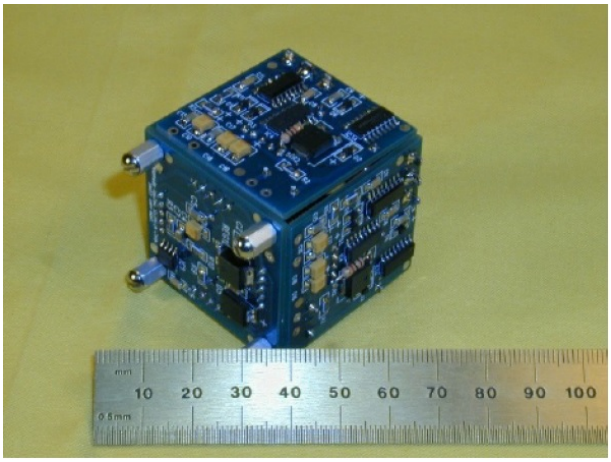

Figure 2.4: 4 Vacuum Arc thrusters mounted onto one side the University of Illinois Cubesat

purpose of calculating the moments generated the thrusters are considered to be on/off thrusters and work in pairs. This results in a set moment being generated for any maneuver.

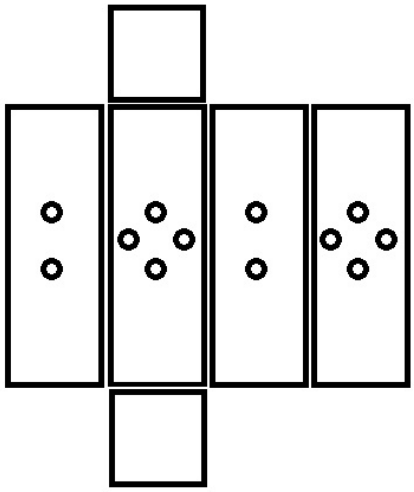

Figure 2.5: Proposed thruster layout of for attitude control on a 3U cubesat. The circles represent the positions of the micro-thrusters on the side of the cubesat.

3 NAVIGATION

3.1 Basic overview

The navigation portion of the GNC is used to provide information for the Control and Guidance portions of the satellite. If the navigation filters are unable to provide accurate information, the satellite will be unable to automate its response or even do simple corrections in its maneuvers. The navigation filter uses the sensors, along with knowledge of the satellites dynamics to predict the next states to allow for more accurate commands from the controller.

3.2 Filtering

The navigation filter is used to provide information for the controller and guidance portions of the GNC. This information is used to determine the current state by providing an estimate. This estimate, provided that the sensor data is accurate enough will eventually converge to provide estimates that are close to the actual state. This is useful if the sensor data is unable to provide information continuously.

The Extended Kalman Filter (EKF) is slightly different from the Kalman filter due to the usage of nonlinear equations as opposed to linear equations of the Kalman Filter. Figure 3.1, shows the general flow of a standard EKF.

The equations used in the general form is as follows:

$$\dot{\mathbf{x}} = \mathbf{f}(\mathbf{x}, \mathbf{k}) + \mathbf{w}(k) \tag{3.1}$$

The equation above is the non-linear state-space form with $\mathbf{f}$ is the function of the past state. $\mathbf{w}$ is the process noise that occurs to the modeled object such as errors. It would be here that errors from additional factors not taken into account from the dynamical model can be added. $\mathbf{x}$ is the input and $\mathbf{k}$ is the time index[51].

$$\mathbf{z}_k = \mathbf{h}_k(\mathbf{x}_k) + \mathbf{v}_k \tag{3.2}$$

The equation shown was the modeled measured output with $\mathbf{h}$ as the nonlinear function for the output of the measured data/output of the model. $\mathbf{v}$ is the noise that occurs to the output of this function such as sensor errors. With the basic equations of the measurement model and the dynamical model ready it is then possible to start propagating for the next time step. However to propagate the nonlinear functions either one has to linearize the equations or find the Jacobians of

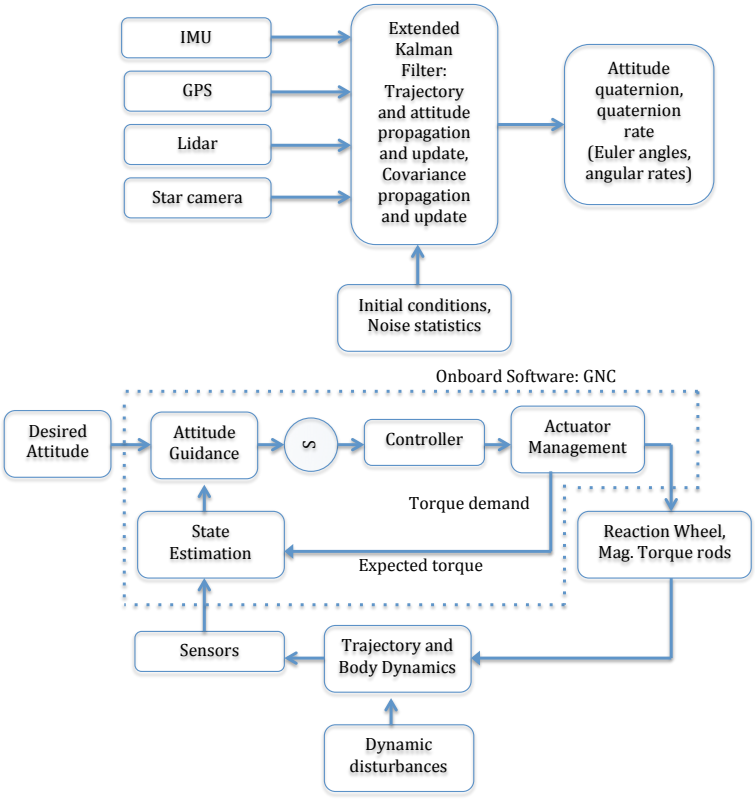

Figure 3.1: The EKF block diagram

the nonlinear functions[51].

$$\mathbf{F}_k = \frac{\delta \mathbf{f}}{\delta \mathbf{x}|_{(x,u,k)}} \tag{3.3}$$

$$\mathbf{H}_k = \frac{\delta \mathbf{h}}{\delta \mathbf{x}}|_{(x,u,k)} \tag{3.4}$$

With the Jacobians found it is then possible to propagate with:

$$\hat{\mathbf{x}}_k^- = \mathbf{f}(\hat{\mathbf{x}}_{k-1}, \mathbf{u}_k, \mathbf{k}) \tag{3.5}$$

$$\mathbf{P}_k^- = \mathbf{F}_{k-1}\mathbf{P}_{k-1}\mathbf{F}_{k-1}^T + \mathbf{Q}_k \tag{3.6}$$

Where $\mathbf{Q_k}$ is the covariance of the process and $\mathbf{u}_k$ is the control forces and torques acting upon the system.

Once the propagation is done, a correction step is needed to update the estimate[51].

$$\mathbf{K}_k = \mathbf{P}_k^- \mathbf{H}_k^T (\mathbf{H}_k \mathbf{P}_k^- \mathbf{H}_k^T + \mathbf{R}_k)^{-1} \tag{3.7}$$

$$\hat{\mathbf{x}}_k = \hat{\mathbf{x}}_k^- + \mathbf{K}_k(\mathbf{z} - \mathbf{h}(\hat{\mathbf{x}}_k^-)) \tag{3.8}$$

$$\mathbf{P}_k = (\mathbf{I} - \mathbf{K}_k \mathbf{H}_k)\mathbf{P}_k^- \tag{3.9}$$

3.3 Internal Measurement Unit

The Inertial Measurement Unit, also known as the IMU is a sensor that can measure angular displacement and rate of an object. This sensor would be placed in a satellite to determine the rotation rate and acceleration due to non-gravitational forces.

The primary means of an IMU to determine the angular rate is through the use of a gyro and accelerometers.

3.3.1 Gyro Model

Gyro Errors

Sensor data from the Gyro is often affected by errors. These errors can range from many different causes, but they can be often be included into the measurement model if the errors are known. They can range from Scale factor errors, misalignment, bias, and other errors. For this simulation, the errors that were taken into account were the scale factor, misalignment, bias, and noise error.

The Angular rate scale factor error is due to the fact that there is a conversion in the gyro that translates the voltage pulses of the gyro into the measurement (radians). This results in an error that is linear and can be seen in the equation below:

$$\Delta\boldsymbol{\Omega}_g = \mathbf{S}_g \boldsymbol{\Omega}_c$$

where

$$\Delta\boldsymbol{\Omega}_g = \begin{bmatrix} \delta\omega_{gx} \\ \delta\omega_{gy} \\ \delta\omega_{gz} \end{bmatrix}$$

$$\mathbf{S_g} = \begin{bmatrix} s_{g1} & 0 & 0 \\ 0 & s_{g2} & 0 \\ 0 & 0 & s_{g3} \end{bmatrix}$$

$$\mathbf{s}_{gi} = \frac{\varepsilon_i}{m_i},$$

The value of each of the $\mathbf{s}_{gi}$ are created with the covariance sigmas of the scale factor error multiplied by a normalized Gaussian random number.

Next is the misalignment error which is due to the placement of the sensor. It is highly probable that there is some misalignment of the sensor in respect to the reference frame, in this case the body of the satellite. This error also can take into account the fact that the sensor is not perfectly orthogonal

Assuming that the misalignment is small, small angle approximations can be used to simplify the equation.

$$\mathbf{\Delta\Omega_{g,axes}} = \mathbf{\Gamma_g \Omega_c},$$

where $\mathbf{\Gamma}_g$ misalignment matrix.

Bias error is due to how the IMU models has a constant error that affects the results. This error is multiplied by a normalized Gaussian random number and added to the results. It uses the axial bias covariance sigmas of the IMU to determine this error.

$$\mathbf{B}_g = \begin{bmatrix} \sigma_{bx}\, n_1 \\ \sigma_{by}\, n_2 \\ \sigma_{bz}\, n_3 \end{bmatrix}$$

where each of the σ_{bi} are the axial bias covariance which is then multiplied by a Gaussian random number n_i.

And finally the Noise error which is due to the random white noise that affects the sensor. These numbers in the simulation are multiplied by a normalized Gaussian random number to create the white noise that affect the results of the sensor.

If the Power Spectral Density (PSD) is known the covariance can be determined via:

$$\sigma_{\omega_i} \approx \frac{PSD_{\theta i}}{\sqrt{\Delta t}},$$

However during this simulation the covariance of the sensor is known for the noise error, thus the $\sigma_{\omega i}$ can be inserted into the equation below without the need to know for find the PSD.

$$\mathbf{E}_g = \begin{bmatrix} \sigma_{\omega x}\, n_1 \\ \sigma_{\omega y}\, n_2 \\ \sigma_{\omega z}\, n_3. \end{bmatrix}$$

Once each of the errors is known, the end results can be adjusted by adding in a total rate error. After that the errors can be added to the results of the sensor simulation

$$\Delta\mathbf{\Omega}_g = \mathbf{S}_g\mathbf{\Omega}_c + \mathbf{\Gamma}_g\mathbf{\Omega}_c + \mathbf{E}_g + \mathbf{B}_g. \tag{3.10}$$

3.3.2 Gyro Measurement Model

Once the errors are known for the Gyro, they can be included with the general Gyro Measurement. For the case of this simulation assumes that the errors are small, thus the model of the Gyro is:

$$\omega_{\mathbf{m}} = \omega_{\mathbf{c}} + \mathbf{\Gamma_g}\omega_{\mathbf{c}} + \mathbf{S_g}\omega_{\mathbf{c}} + \mathbf{B_g} + \mathbf{E_g}, \tag{3.11}$$

or

$$\omega_{\mathbf{m}} = \omega_{\mathbf{c}} + \mathbf{\Delta\Omega_g}. \tag{3.12}$$

where ω_c is the true angular velocity of the satellite. This angular velocity is calculated by differentiating the angular rotation of the satellite in comparison to the previous time step's angular position.

$$\omega = \frac{\mathbf{\Delta}\alpha}{\mathbf{\Delta t}}.$$

3.4 Conventional attitude sensors

Inertial Measurement Unit (IMU), GPS receivers, star camera and Magnetometer are used on a satellite to conduct measurements and to determine position, velocity, acceleration, attitude angles, angular rates and magnetic field vector. IMU provides non-gravitational acceleration measurements and angular-rate measurements. Star camera is used to determine spacecraft attitude using camera pictures and star catalog

GPS receiver data are utilized to compute spacecraft position and velocity with respect to inertial coordinate system.

Generally, the attitude is controlled by implementing a closed-loop control and utilizing micro-thrusters, reaction wheel and three magnetic torque rods.

All measurements and operations to compute the state vector are performed on-board and communicated with ground-based mission operations center.

3.4.1 Attitude sensors with navigation solutions

There exist attitude sensors that are costly and provide navigation solutions for flight vehicles. But these solutions require integration with control algorithms. The sensors described below are some examples of hardware items with Kalman filter algorithms for an onboard GNC execution. **IG-500A system**. The IG-500A is a miniature Attitude and Heading Reference System (AHRS) (Fig. 3.2). It uses a set of three MEMS based gyroscopes, accelerometers, and magnetometers, to provide a drift-free and precise attitude, even in severe dynamic conditions. This lightweight, robust and reliable device delivers consistent information over a wide temperature range thanks to an advanced calibration procedure and a configurable Extended Kalman filter (EKF).

Figure 3.2: A miniature Attitude and Heading Reference System: G-500A

MIDG SERIES INS/GPS system. MIDG SERIES INS/GPS is an Inertial Navigation System (INS) with Global Positioning System (GPS) which provides the inertial navigation solution (Fig. 3.3). Operational modes are selectable, including IMU only operation, vertical gyro simulation with magnetic aiding, and full INS solution. It is intended for use in applications that require a full state vector, including attitude, position, altitude, velocity, acceleration, and angular rates. The system features are as follows:

size: 1.50 x 1.56 x 0.88,
weight: under 55 grams, includes a
3-Axis Rate Gyro,
3-Axis Accelerometer,
3-Axis Magnetometer, and
differential ready GPS.
Power input is 10 to 32 VDC, 1.2W maximum.

The system facilitates estimation of the state (position, velocity, and attitude) using Kalman Filter at 50Hz.

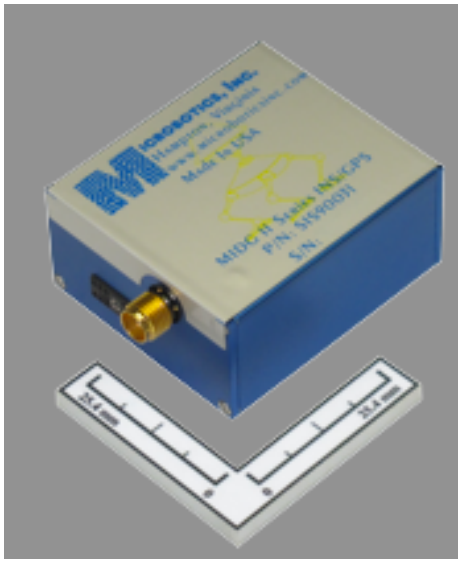

Figure 3.3: MIDG SERIES INS/GPS system

The proposed GNC system uses Extended Kalman Filtering algorithms integrated with guidance and control functions. Therefore, this system and its utility is advantageous in terms of accuracy of navigation solutions and integration with other GNC subsystems compared to those of the sensor systems described above.

4 CONTROL

This section will primarily cover control systems and the method used in the simulation. In particular, the control system used is for the attitude of a small spacecraft using thrusters. Thus the commands sent to the actuators after the controller determined the desired output needed to be adjusted for on/off commands.

Due to the various factors that affect the system along with the nonlinear equations of motion, a nonlinear control system is used. In particular a control system was needed to work in conjunction with the guidance and navigation to create an autonomous system to reach the desired state. [32]

The controller is a PD controller which then outputs its commands into an actuation unit. From there the system determines how to use the actuators within the limits of the thrusters. Since the thrusters are on/off systems and are fixed the actuation of the system needs to take this into account. Thus the thrust management needs to be done in the actuation commands.

Within this chapter, a control system will be shown and designed to work with the outputs of the Guidance and Navigation portions from the previous sections. It will then cover how these control outputs are then sent to the actuators which then affect the dynamical system, thus taking the system back to the Navigation stage.

4.1 Definition of Control

The purpose of a control system is to provide the commands that are used by the actuators to correct or adjust the current state of the system to the desired state. As is mentioned by Fehse, the controller uses the Navigation and Guidance portions to determine an error and then generates a command to fix the error [35].

The controller function contains two primary functions. First is the controller which provides the control errors and the commands to the actuator. Second is the Actuator management which translates the controller commands from force and torque into on or off commands [35]

4.2 Control Law

Control laws are used to determine the necessary input to a system to achieve a desired result. For the purpose of this simulation a Proportional, Differential (PD) controller was used to determine the moment that is needed for the system. As seen below in equation 4.1 the controller uses the Guidance output and uses the properties of the errors to create an output which is then

interpreted and sent to the actuators.

$$\mathbf{T}_{PD} = \mathbf{k}_p \cdot (\mathbf{e}) + \mathbf{k}_d \cdot \left(\frac{\Delta \mathbf{e}}{dt} \right) \tag{4.1}$$

$$e = desiredstate - currentstate \tag{4.2}$$

where k_p is the proportional gain, k_d is the derivative gain, and the output $\vec{T}_{PD}$ is the PD controller's commanded torque. In the case of determining the gains for the Controller, trial and error was the primary method used. It was found that the gains would need to be set extremely small in order to prevent the satellite from constantly over compensating for the small errors. This was exacerbated by the fact that all calculations were done in radians as opposed to degrees. As a result the difference between the current position and the targeted position would become extremely small, and add to the fact that the thrusters used were produced force in the micro-Newtons, scaling became key.

What had been found was that if the gains were too high, the system would become undamped as the controller would over compensate. Early simulations ran into this problem before eventually the current gains were found. Examples of this issue could be seen in various papers such as in Min's paper where the thruster command would be constantly firing on and off [10]. This was caused by the systems inability to zero out it's velocity with its thrusters, thus unable to maintain its desired position. This could either be fixed by including an actuator that is not dependent on a switch logic.

For the simulations that were done the gains were set to the values seen below in table 4.1. With the gains set to these values the resulting system is underdamped. Though this allows for some overshoot of the target value, it also allows for faster acquisition of the target state for the current simulations.

k_p	.0003
k_d	.0259

Table 4.1: Controller Gain Values

4.3 Actuation commands

Once the controller has determined the command it sends to the actuation unit, the system needs to process it into a command that is feasible by the system. Often times the actuators used, like the thrusters are only capable of on/off operations. Thus the actuation commands use various systems such as the bang-bang control system, pulse-width pulse-frequency (PWPF) modulation[10], along with many other variations [52].

Boundary condition for positive torque	5.4 μN*m
Boundary condition for negative torque	-5.4 μN*m

Table 4.2: Thruster boundary conditions

Given that the thrusters are meant to be used only for attitude actuation, they are kept as pairs to create a moment. The commands from the controller are checked to see if they exceed a threshold. If for that time step the controller's output exceeds the threshold, the actuator will activate and stay active until the controller output no longer exceeds it. As the controller and sensors follow a standard time-step, there are instances where the system is unable to fully stabilize itself as will be seen in the results section.

As a result the thrusters will activate once the commanded torque sent to the actuation manager exceeds a specified amount. Given that the command is sent as a function of angular acceleration, the system converts it into torques, upon which, if it exceeds the specified limit as seen in Table 4.2, then the specified sets will activate. Otherwise the thruster pairs will remain inactive. Given that the torques generated for each axis is the same due to the thruster layout, the conditions for each rotation axis is identical. This can be changed if necessary.

Due to the continuing miniaturization, systematization and complication trend of SS missions, onboard propulsion systems are now expected to provide more precision impulse as well as achieving lower volumes and power consumptions. Microelectromechanical systems (MEMS) techniques offer great potential in satisfying the mission requirements for the next generation of micro propulsion systems. Thus since the 1990-s, a number of research organizations, such as NASA, JPL, TRW, ESA, have focused their attention towards the design and fabrication of MEMS based micro propulsions, among which solid propellant micro propulsions are proved to be more applicable for the orbit adjustment and attitude control of small satellites [40]-[53].

Electrically controlled extinguishable solid propellants (ESCSP) are capable of multiple ignitions, extinguishments and throttle control by the application of electrical power. The simplicity of these thrusters will enable their broad use on micro-pico satellites for primary propulsion, ACS and formation flying applications [54].

The NANOsatellite Propulsion System (NANOPS) is part of the CanX-2 (Canadian Advanced Nanospace eXperiment 2) mission to demonstrate enabling component technologies in support of future formation flying missions. The target performance goals are 50 mN of thrust, a specific impulse of 45s, and a minimum impulse bit of 0.0005 Ns. The CanX-2 experiment will mainly involve attitude control maneuvers in order to evaluate the performance of the propulsion system through on-board attitude sensors [55] . Colloid Thruster for Attitude Control Systems (ACS) have the following features:

- Colloid N thrusters delivering 5 to 30 N each

- Thrust controllability and resolution 0.1 N

- Thrust noise $0.1N/Hz^0.5$ from 1 to 30 mHz

- 4 thrusters/cluster, 2 clusters for mission with duration of 3 months (2200 hours) [56].

A Novel Cold Gas Propulsion System has been developed for Nanosatellites and Picosatellites. An example of such system is Micro-Electromechanical-based PICOSAT Satellite Inspector (MEPSI) [57], [58].

Micro RF Ion Engine for Small Satellite Applications has demonstrated 1.4-2.1 mN thrust and 1500-2850 sec Isp with 70-110 total power (RF + ion beam power) . Applications are

- Formation flights, Spacecraft initial stabilization, Station-keeping and active drag compensation, Onboard on a micro-satellite with 50 kg wet mass. Propulsion system dry mass 3 kg, Nominal performance at 2-mN thrust and 2500-sec Isp [59].

Other types of thrusters include green, electrical, pulsed plasma, hydrazine, propulsion systems [60]-[53]. The green propulsion is emerging as an viable alternative to Hydrazine with higher performance, enhanced volumetric efficiency and reduced risks.

In particular, in Ref. [61] 3U Cubesats are considered on a nominal 600Km altitude orbit:

-3U Cubesat mass is 3 kg. Hence the whole thruster assembly will be limited to 150 g.

-The propellant (Teflon) mass will be limited to 10g.

- The total impulse needed to fully compensate three years of drag will be 28.4Ns.

-Considering a propellant mass of 10g, translates into a minimum Isp of 290 s.

-Maximum average power consumption limited to 0.3 W.

5 GUIDANCE

The Guidance of a GNC system is to determine the path that the system will take to achieve its goal. In the case of the system used here, a polynomial function was derived from the E-Guidance to create a guidance formula. This system is a derivation of the Guidance system used in the Apollo landings for position, thus needed to be adapted to work in a 3 axis attitude system.

Based upon the Apollo lunar landing, the guidance law used is based upon the e-guidance law, however it derives it down to a polynomial..

Guidance laws. The *original and general concept of guidance*, obtained first by George Cherry, a MIT staff member, and known as the explicit (E)-guidance, is given by formula:

$$\mathbf{a}_{com} = \mathbf{c}_1(\mathbf{x}_c, \mathbf{x}_d)p_1(t) + \mathbf{c}_2(\mathbf{x}_c, \mathbf{x}_d)p_2(t) - \mathbf{g}$$

where $\mathbf{a}_{com}$ is the commanded *translational* acceleration, $\mathbf{x}_c$ and $\mathbf{x}_d$ are the current (”c”) and desired (”d”) (target) states, and $\mathbf{g}$ is the gravitational acceleration, and p_1 and p_2 are arbitrary functions of time [36]. As mentioned in Chapter 1, Alan Klumpp, an Apollo engineer, adjusted this formula to obtain his quartic polynomial- based lunar descent guidance formula, which then was implemented in all Apollo missions. A thrust acceleration to be commanded at any point in space consists of three terms: the acceleration of the reference trajectory at a particular time, minus two feedback terms proportional to velocity and position deviations from the reference trajectory [37].

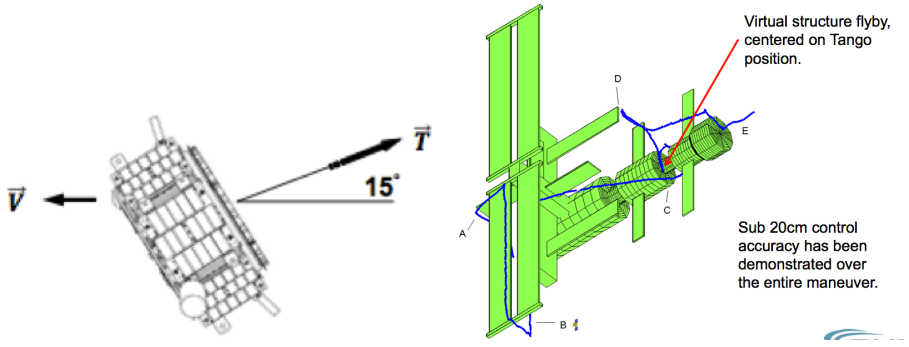

Figure 5.1: FASTRAC and PRISMA satellite systems.

The proposed research modifies Klumpp’s polynomial guidance law by using a PD control law and extends it from a ground-based, pre-mission trajectory guidance to real-time attitude guidance for an onboard execution. The proposed polynomial guidance computes the

commanded angular accelerations using the differences between the current and desired values of the attitude parameters.

5.1 Guidance equations for translational motion

Significant portion of the reference landing trajectory can be determined by employing a quartic polynomial formulation. This formulation allows us to satisfy five constraints on the reference trajectory. This trajectory can be constructed backwards from the target point. The position, velocity and acceleration vectors, $\mathbf{R}_{RG},\ \mathbf{V}_{RG},\ \mathbf{A}_{RG}$ on the reference trajectory can be determined in a quartic polynomial formulation: [37]

$$\mathbf{R}_{RG} = \mathbf{R}_{TG} + T\mathbf{V}_{TG} + \frac{T^2}{2}\mathbf{A}_{TG} + \frac{T^3}{6}\mathbf{J}_{TG} + \frac{T^4}{24}\mathbf{S}_{TG}, \tag{5.1}$$

$$\mathbf{V}_{RG} = \mathbf{V}_{TG} + T\mathbf{A}_{TG} + \frac{T^2}{2}\mathbf{J}_{TG} + \frac{T^3}{6}\mathbf{S}_{TG}, \tag{5.2}$$

$$\mathbf{A}_{RG} = \mathbf{A}_{TG} + T\mathbf{J}_{TG} + \frac{T^2}{2}\mathbf{S}_{TG}, \tag{5.3}$$

where T is the target referenced time, the vectors $\mathbf{R}_{TG},\ \mathbf{V}_{TG},\ \mathbf{A}_{TG},\ \mathbf{J}_{TG},\ \mathbf{S}_{TG}$ are position, velocity, acceleration, jerk and snap vectors defined at the target point. Note, that $T = 0$ at the target point, which means that T is negative during the maneuver.

The acceleration to be commanded at any point consists of the acceleration on the reference trajectory, two feedback terms, proportional to position and velocity deviations from the reference trajectory: [37]

$$\begin{aligned}\mathbf{A}_{CG} = {} & \mathbf{A}_{TG} + T\mathbf{J}_{TG} + \frac{T^2}{2}\mathbf{S}_{TG} - \\ & (\mathbf{V}_G - \mathbf{V}_{TG} - T\mathbf{A}_{TG} - \frac{T^2}{2}\mathbf{J}_{TG} - \frac{T^3}{6}\mathbf{S}_{TG})\frac{K_V}{T} - \\ & (\mathbf{R}_G - \mathbf{R}_{TG} - T\mathbf{V}_{TG} - \frac{T^2}{2}\mathbf{A}_{TG} - \frac{T^3}{6}\mathbf{J}_{TG} - \frac{T^4}{24}\mathbf{S}_{TG})\frac{K_R}{T^2},\end{aligned} \tag{5.4}$$

where K_R and K_V are the feedback gains. Eq.(5.4) is the implicit guidance equation. The reference trajectory corresponds to a quartic, but the trajectory, generated by Eq.(5.4) is not a quartic. This equation can be rewritten as a quartic and made as the explicit guidance equation by specifying the feedback gains, K_R and K_V. By regrouping ther similar terms, one can rewrite

Eq.(5.4) in the form: [37]

$$\begin{aligned}\mathbf{A}_{CG} &= -\frac{K_R}{T^2}\mathbf{R}_G - \frac{K_V}{T}\mathbf{V}_G + \\ &\frac{K_R}{T^2}\mathbf{R}_{TG} + \frac{K_R + K_V}{T}\mathbf{V}_{TG} + \left(1 + K_V + \frac{K_R}{2}\right)\mathbf{A}_{TG} + \\ &\left(1 + \frac{K_V}{2} + \frac{K_R}{6}\right)T\mathbf{J}_{TG} + \left(\frac{1}{2} + \frac{K_V}{6} + \frac{K_R}{24}\right)T^2\mathbf{S}_{TG}. \end{aligned} \tag{5.5}$$

Eq.(5.4) can be identified as the second order differential equation:

$$\ddot{x} + 2q\omega\dot{x} + \omega^2 = 0,$$

where $\ddot{x}$ and $\dot{x}$ represent deviations in acceleration and velocity, q and ω are the damping ratio and natural frequency, and K_R and K_V can be associated with these parameters by expressions: [37]

$$K_V = -2q\omega T, \qquad K_R = \omega^2 T^2.$$

By introducing $P = \frac{2\pi}{\omega}$, these expressions are rewritten as

$$K_R = \frac{4\pi^2 T^2}{P^2}, \qquad K_V = -2\sqrt{K_R}q.$$

The gains K_R and K_V can be selected by equating the coefficients of $\mathbf{J}_{TG}$ and $\mathbf{S}_{TG}$ in Eq.(5.5) to zero:

$$1 + \frac{K_V}{2} + \frac{K_R}{6} = 0,$$
$$\frac{1}{2} + \frac{K_V}{6} + \frac{K_R}{24} = 0.$$

By solving these equations for K_R and K_V, it can easily be obtained that

$$K_R = 12, \qquad K_V = -6.$$

Using these values, one can have

$$\frac{P}{T} = -\frac{\pi}{\sqrt{3}}, \qquad q = \frac{\sqrt{3}}{2}.$$

Consequently, Eq.(5.5) is rewritten as

$$\mathbf{A}_{CG} = \frac{12}{T^2}(\mathbf{R}_{TG} - \mathbf{R}_G) + \frac{6}{T}(\mathbf{V}_{TG} + \mathbf{V}_G) + \mathbf{A}_{TG}. \tag{5.6}$$

Let $T_P = T + t_d$, where t_d is transport delay, T_P is the predicted time. The acceleration of the quartic at the predicted time T_P is the acceleration to command at the current time T in order to realize the quartic profile. The constraint for the actual trajectory to be a quartic is given as [37]

$$\begin{bmatrix} \mathbf{R}_G \\ \mathbf{V}_G \end{bmatrix} = \begin{bmatrix} 1 & T & \frac{T^2}{2} & \frac{T^3}{6} & \frac{T^4}{24} \\ 0 & 1 & T & \frac{T^2}{2} & \frac{T^3}{6} \end{bmatrix} \begin{bmatrix} \mathbf{R}_{TG} \\ \mathbf{V}_{TG} \\ \mathbf{A}_{TG} \\ \mathbf{J}_{TA} \\ \mathbf{S}_{TA} \end{bmatrix},$$

where $\mathbf{R}_G$ and $\mathbf{V}_G$ are the current position and velocity vectors on the actual trajectory, and the jerk and snap vectors, $\mathbf{J}_{TA}$ and $\mathbf{S}_{TA}$ are considered as those which would be achieved at the target point on the actual trajectory. These two vectors can be found from this equation in the form: [37]

$$\begin{bmatrix} \mathbf{J}_{TA} \\ \mathbf{S}_{TA} \end{bmatrix} = \begin{bmatrix} -\frac{24}{T^3} & -\frac{18}{T^2} & -\frac{6}{T} & \frac{24}{T^3} & -\frac{6}{T^2} \\ \frac{72}{T^4} & \frac{48}{T^3} & \frac{12}{T^2} & -\frac{72}{T^4} & \frac{24}{T^3} \end{bmatrix} \begin{bmatrix} \mathbf{R}_{TG} \\ \mathbf{V}_{TG} \\ \mathbf{A}_{TG} \\ \mathbf{R}_G \\ \mathbf{V}_G \end{bmatrix}. \tag{5.7}$$

So, the acceleration to be commanded at the current time T and realized at the predicted time T_P is given as

$$\mathbf{A}_{CG} = \mathbf{A}_{TG} + T_P \mathbf{J}_{TGA} + \frac{T_P^2}{2} \mathbf{S}_{TGA}. \tag{5.8}$$

Substitution of Eq.(5.8) into Eq.(5.7) yields

$$\mathbf{A}_{CG} = 12\frac{(3p^2 - 2p)}{T^2}(\mathbf{R}_{TG} - \mathbf{R}_G) + 6\frac{(4p^2 - 3p)}{T}\mathbf{V}_{TG} +$$

$$6\frac{(2p^2 - p)}{T}\mathbf{V}_G + (6p^2 - 6p + 1)\mathbf{A}_{TG}, \tag{5.9}$$

where $p = \frac{T_P}{T}$. When $T_P = T$ and $t_d = 0$, Eq.(5.9) becomes identical to Eq.(5.6).

5.1.1 Commanded thrust acceleration for translational motion

First, let's compute the ratio of the predicted target referenced time to the current target referenced time [37]:

$$T_{PT} = \frac{TTT + t_{LEAD}}{TTT},$$

where TTT is the target referenced time, t_{LEAD} is transport delay. Then the acceleration to be commanded at the current time TTT and realized at the predicted time T_{PT} can be computed as follows [37]

$$\mathbf{A}_{CG} = 12\frac{T_1}{TTT^2}(\mathbf{R}_{TG} - \mathbf{R}_G) + 6\frac{T_2}{TTT}\mathbf{V}_{TG} + 6\frac{T_3}{TTT}\mathbf{V}_G + T_4\mathbf{A}_{TG}, \tag{5.10}$$

where

$$\begin{aligned} T_1 &= 3T_{PT}^2 - 3T_{PT}, \\ T_2 &= 4T_{PT}^2 - 3T_{PT}, \\ T_3 &= 2T_{PT}^2 - T_{PT}, \\ T_4 &= 6T_{PT}^2 - 6T_{PT} + 1. \end{aligned}$$

Commanded unit thrust vector.

The commanded unit thrust vector is defined directly from the commanded thrust acceleration vector determined in (5.10) as follows:[37]

$$\mathbf{A}_{CP} = (\mathbf{T}_P^G)^T\mathbf{A}_{FCG}, \tag{5.11}$$

$$\mathbf{A}_{FCP} = \mathbf{A}_{CP} - \mathbf{G}_{MP}, \tag{5.12}$$

$$\mathbf{U}_{FCP} = \textbf{unit}[\mathbf{A}_{FCP}]. \tag{5.13}$$

5.2 Guidance equations for angular motion

Converting the Guidance equations from translation motion to angular motion was a matter of converting the equations of motion. By using the similarities between translational and angular equations of motion, it was possible to make a simple conversion. By using vectors $\alpha_{\mathbf{TG}}$, $\mathbf{\Omega_{TG}}$, $\dot{\mathbf{\Omega}}_{\mathbf{TG}}$ in place of $\mathbf{R}_{TG},\ \mathbf{V}_{TG},\ \mathbf{A}_{TG}$ in equation 5.6 which results in 5.14.

$$\epsilon_{CG} = \frac{12}{T^2}(\alpha_{TG} - \alpha_G) + \frac{6}{T}(\mathbf{\Omega}_{TG} + \mathbf{\Omega}_G) + \dot{\mathbf{\Omega}}_{TG}. \tag{5.14}$$

where:

- ϵ_{CG} is the angular acceleration guidance command to be used to compute angular acceleration increments for the actuators.

- $\dot{\mathbf{\Omega}}_{TG}$ is the targeted acceleration. This acceleration is determined by the PD controller.

- α_{TG} and α_G is the targeted angular position and reference position respectively.

- $\mathbf{\Omega}_{TG}$ and $\mathbf{\Omega}_{G}$ is the targeted angular velocity and the reference angular velocity respectively.

- $\mathbf{T}$ is the target referenced time.

As Klumpp made note in his paper on the Apollo landing, the commanded guidance has three major parts. The acceleration of the reference trajectory (aka our PD controller input), the velocity and positional deviations from the reference trajectory feedback [37].

The real-time targeting procedure implies on-board computations of the target states, namely, position, velocity, angle and angular rate vectors, and the time remaining to achieve the target state from the current state. The targeting is performed as many times as needed depending on the necessity of changing the target state. If no changes are made, then the target state becomes the final state. As is used below, the target states play a critical role in the computation of the commanded angular acceleration, the guidance command. Therefore, the integrated real-time targeting and re-targeting procedures are an integral part of the on-board guidance subsystem and the GNC system. That is why the guidance considered in this work is referred to as the ”target-relative guidance”. One of the advantages of the existence of the closed-form solutions for attitude control is that they allow us to conduct real-time targeting at any given time during the guided maneuver. In this work, since the circular orbit is considered as a reference orbit, the target state includes all Euler angles and their rates.

In this work, in particular, the target state components are calculated in real time, based upon the current reference position and velocity, and angle and angular rates. For simple maneuvers the targeted angular position and velocity are either the final desired outcome, or are calculated beforehand on the ground before the maneuver of interest is performed [37, 62, 63]. In the case of the automated system, since the outcome is not dependent of reaching at set point at a set time, and the end velocity and acceleration is zero, the targeted points are the same as the goal (final) states.

In the case for more complex maneuvers, such as a moving target, the guidance target would need to recalculate often. In the case for this simulation, the targeting calculation is done with every measurement input due to the simplicity of the operation. In this case the targeting is updated every 0.2 seconds along with the control outputs from the PD controller. Depending on the targeting algorithms the satellite can then follow a series of targets with specified conditions such as desired angular velocities for the sake of tracking an object.

6 SIMULATIONS

6.1 Satellite and orbit properties

The simulation of the GNC system used the properties of a 3U cube sat. The satellite's moment of inertia is shown in 6.1:

.

I_{xx}	0.033
I_{yy}	0.0067
I_{zz}	0.033

Table 6.1: 3U cubesat moments of inertia

The micro-thrusters used for this simulation can also be seen in Table 6.2. These micro-thrusters were used are based upon the University of Illinois vacuum arc thruster that had a thrust of 54 μN. The Arc thrusters were also stated that when paired for use on a Cubesat, created a moment of 5.4 μNm. In Table 6.3, the boundary conditions for the thrusters are seen. These conditions are compared to the converted torque from the commanded acceleration from the guidance command.

.

T_{xx}	5.4 μNm
T_{yy}	5.4 μNm
T_{zz}	5.4 μNm

Table 6.2: Torques produced by Arc Thrusters

The use of equal angular torques from the thrusters was primarily for simplification of the tests. Given that Cubesats are built around modules that are 10 x 10 x 10 cm, the assumption was then that the central module/section of the Cubesat contained the thrusters.

As for the orbital elements, the satellite is considered to be in a geostationary orbit with the parameters given in table 6.4. It should be noted that the satellite is also assumed to be orbiting about the equator. These assumptions were made to allow a greater focus on the attitude GNC.

Boundary condition for positive torque	5.4 μN*m
Boundary condition for negative torque	-5.4 μN*m

Table 6.3: Thruster boundary conditions

.

r	42211 km
v	3.07 km/s

Table 6.4: Orbital elements

The desired final conditions for these simulations will be to reach a zeroed position as seen in Table 6.5. For now the simulation focuses on smaller angular motions, primarily due to the use of Euler angles. This reduces the risk of the simulation hitting a Gimbal lock.

.

Pitch Pos	0 deg
Pitch Vel	0 deg/s
Roll Pos	0 deg
Roll Vel	0 deg/s
Yaw Pos	0 deg
Yaw Vel	0 deg/s

Table 6.5: Satellite final targeted angular position and velocity for both maneuvers: reorientation, and de-tumbling and reorientation

6.2 Reorientation: initial conditions

The first simulation was a simple maneuver based upon reorienting the satellite towards a specific direction. The inital conditions for this satellite will have no initial angular velocity or acceleration. The only difference from the satellites initial to final conditions will be its position. These initial conditions can be seen in Table 6.6.

.

Pitch Pos	3 deg
Pitch Vel	0 deg/s
Roll Pos	-3 deg
Roll Vel	0 deg/s
Yaw Pos	-1.5 deg
Yaw Vel	0 deg/s

Table 6.6: Satellite starting angular position and velocity for reorientation

6.3 De-tumbling and Reorientation: initial conditions

The next simulation is based around the satellite having an initial angular velocity. Thus the satellite needs to reduce or use its initial angular velocity to work towards it final desired position. Within Table 6.7, the initial conditions can be seen. As like the previous simulation, the final desired conditions are listed in Table 6.5.

Pitch Pos	1 deg
Pitch Vel	0.3 deg/s
Roll Pos	1 deg
Roll Vel	-0.2 deg/s
Yaw Pos	-2 deg
Yaw Vel	0 deg/s

Table 6.7: Satellite starting angular position and velocity for detumbling and reorientation

7 RESULTS

7.1 Reorientation

During this simulation the satellite was reoriented from its starting position where it was offset as seen in the previous section's table 6.6. The satellite starts offset by a few degrees from its desired position at 0 degrees in all axis.

Seen in Figure 7.1, the satellite's pitch moves towards zero. Figure 7.2 shows that the satellite has a starting angular velocity in the pitch axis of zero, thus in Figure 7.3 the commanded acceleration is shown to act to reorient the satellite's pitch so that it reaches its goal of 0 degrees.

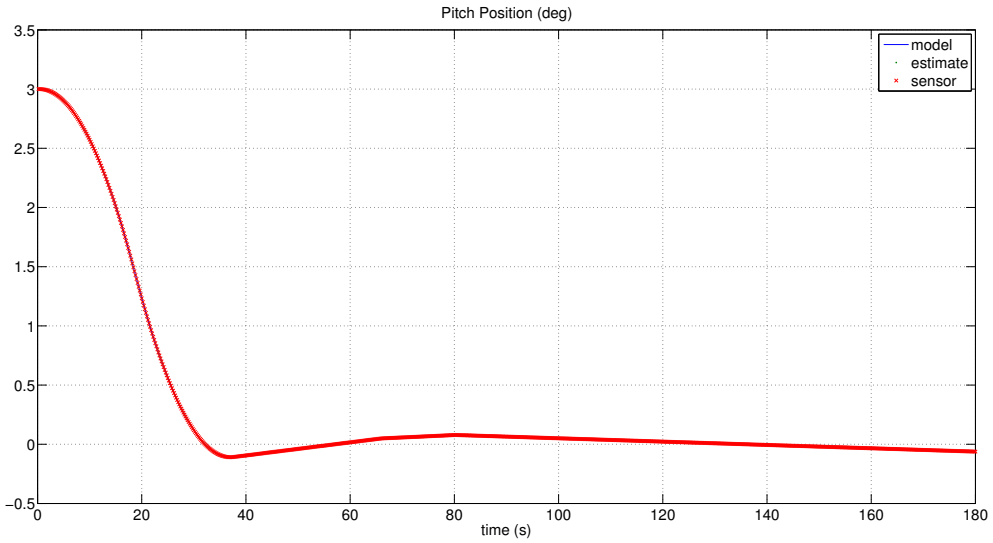

Figure 7.1: The pitch position of the satellite in relation to time. Note that the position starts offset at 3 degrees and eventually reaches close to zero.

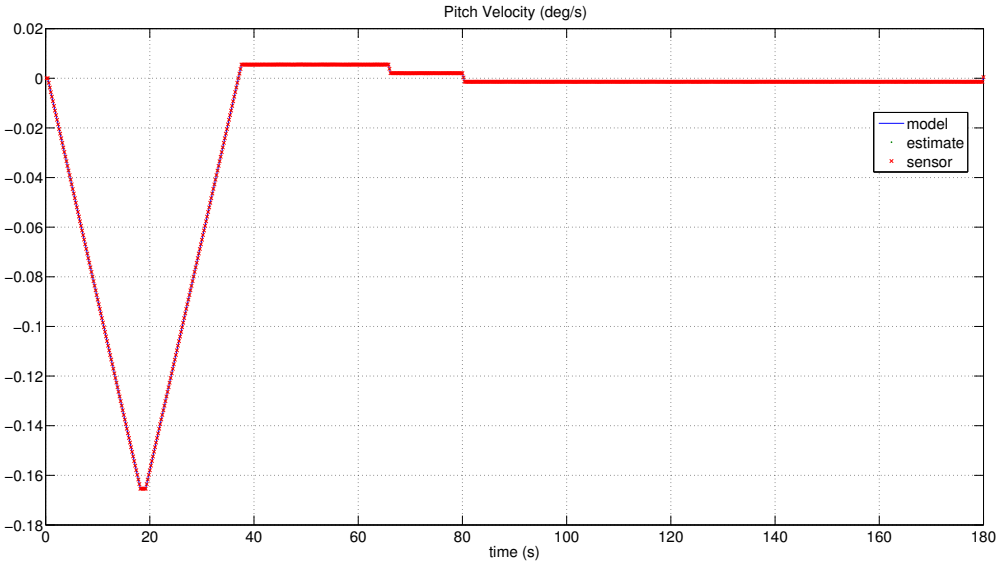

Figure 7.2: The pitch velocity of the satellite in relation to time. This case starts with an angular velocity of zero and ends close to zero.

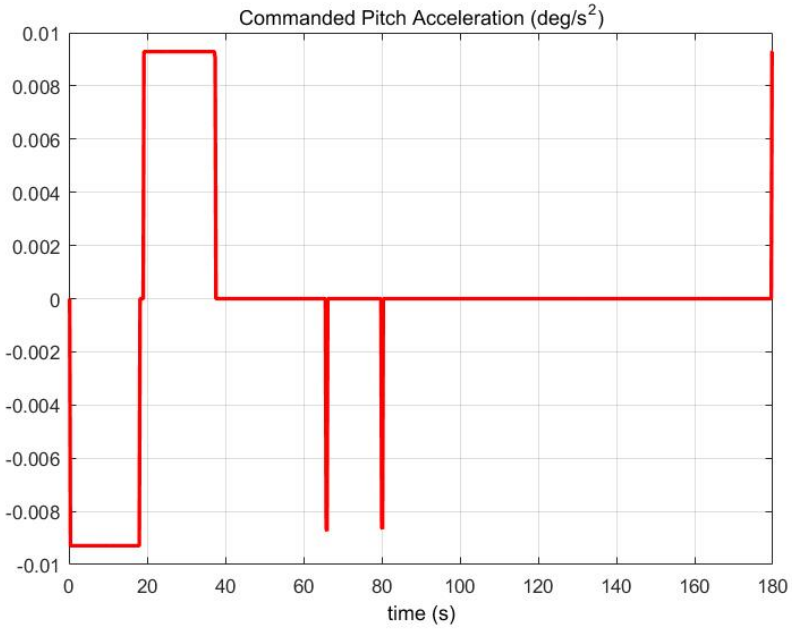

Figure 7.3: The commanded pitch acceleration in relation to time. The satellite's thrusters are primarily used at the start of the maneuver and only are used twice afterwards to stabilize the position.

In Figure 7.4, the roll position is shown just as seen in the previous figures. The starting position as noted earlier in Table 6.6 is 3 degrees. The end goal is 0 degrees which is nearly

achieved at 40 seconds after which the satellite stays within 0.1 degrees. In Figure 7.5 the angular velocity of the roll is shown starting from zero, upon which it accelerates up until approximately 20 seconds, upon which it starts to decelerate to prevent overshooting its target position. Figure 7.6 shows how the commanded acceleration of the roll is acting upon the system. After the first 40 seconds, the only acceleration that is used is to prevent the satellite from deviating more then 0.1 degrees from its targeted point.

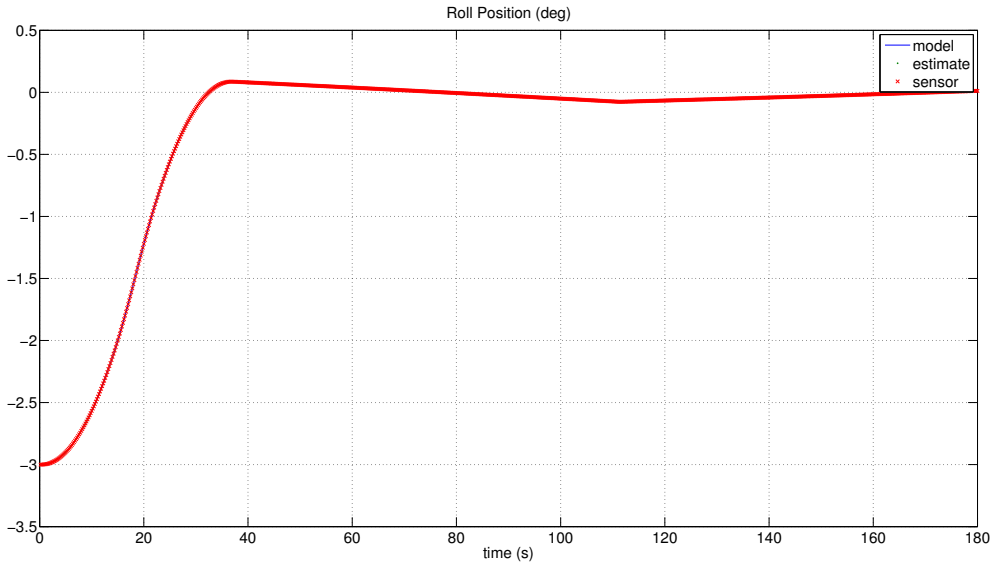

Figure 7.4: The angular position of the satellite's roll in relation to time. Note that the angle starts at -3 degrees and ends close to 0 degrees.

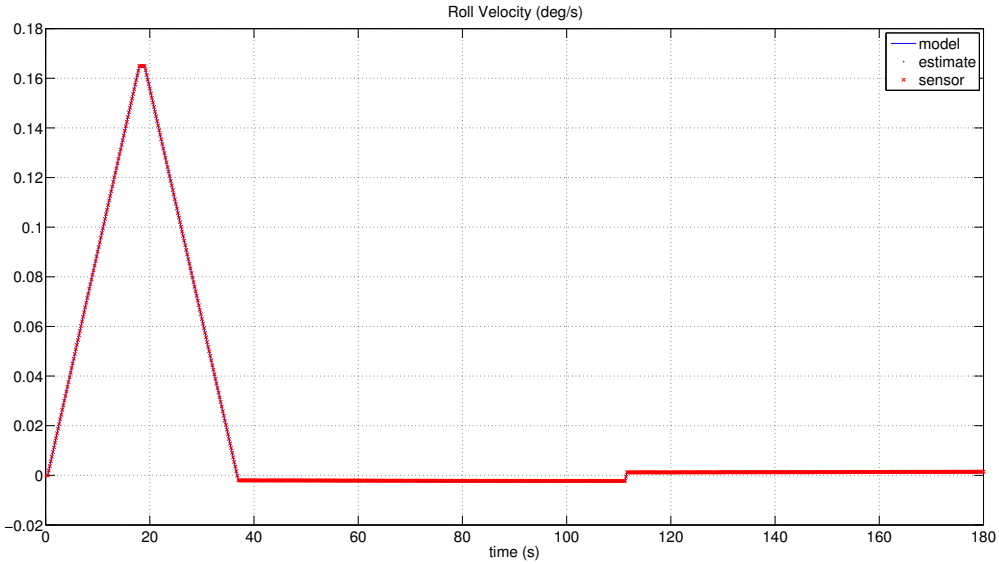

Figure 7.5: The angular velocity of the satellite's roll in relation to time. Note that the angular velocity started at 0 degrees per second and ends close to 0 degrees per second.

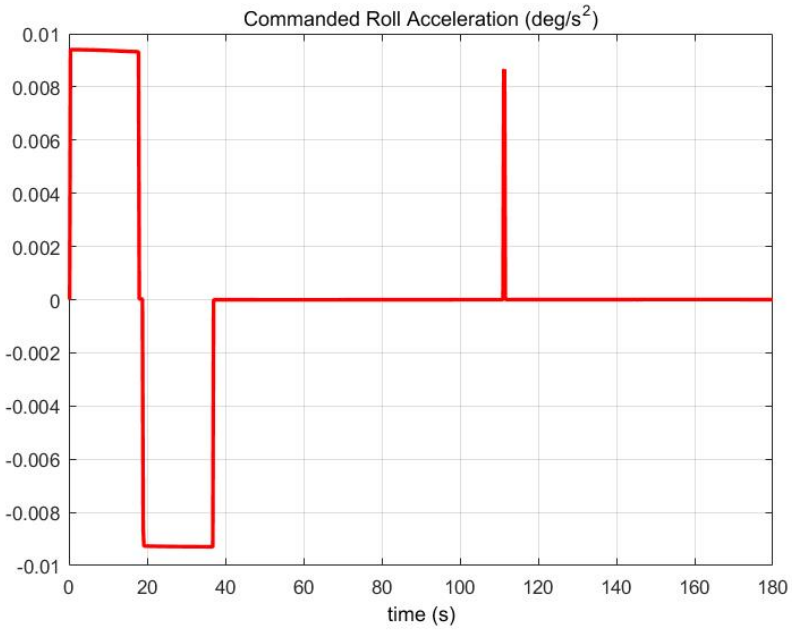

Figure 7.6: The angular acceleration of the satellite's roll in relation to time. Note that the angular acceleration tries to use the least amount of thrust to reduce fuel consumption. When compared to Figure 7.14 the affects the thrust has on the velocity can be easily seen.

Figure 7.7 shows the yaw position of the satellite. This time it starts at -1.5 degrees and makes its way up to 0 degrees. Like the previous figures it is shown that the angular position once

it gets close to its target point, stays within a 0.1 degree deviation. Figure 7.8 shows the angular velocity. Unlike 7.5 where the velocity is descending at a constant rate due to the constant use of the thruster as seen in Figure 7.6, the velocity is in a more step like pattern. This is due to the commanded acceleration as seen in Figure 7.9 not constantly used during the deceleration stage. This is primarily due to how the controller and guidance coefficients not pushing the command beyond the threshold value to keep the thrusters on constantly during this time period.

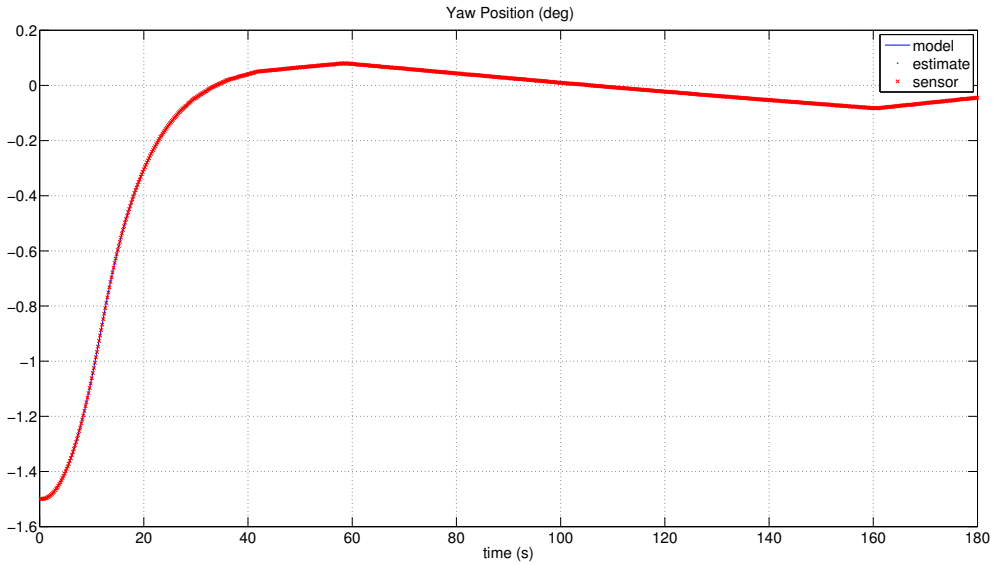

Figure 7.7: The angular position of the satellite's yaw in relation to time. Note that the angle started at -2 degrees and ends at 0 degrees.

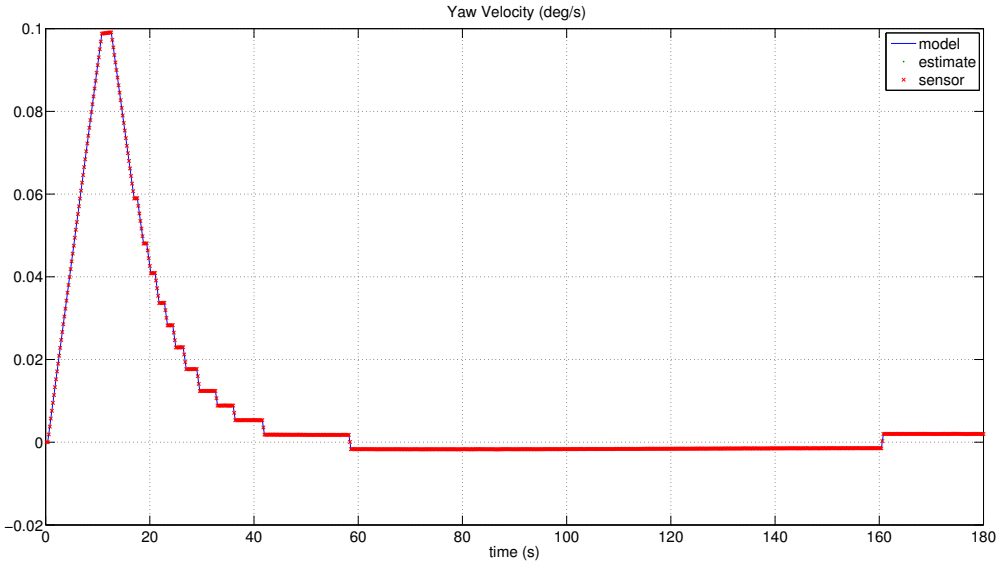

Figure 7.8: The angular velocity of the satellite's yaw in relation to time. Note that the angular velocity started at 0 degrees per second and ends close to 0 degrees per second.

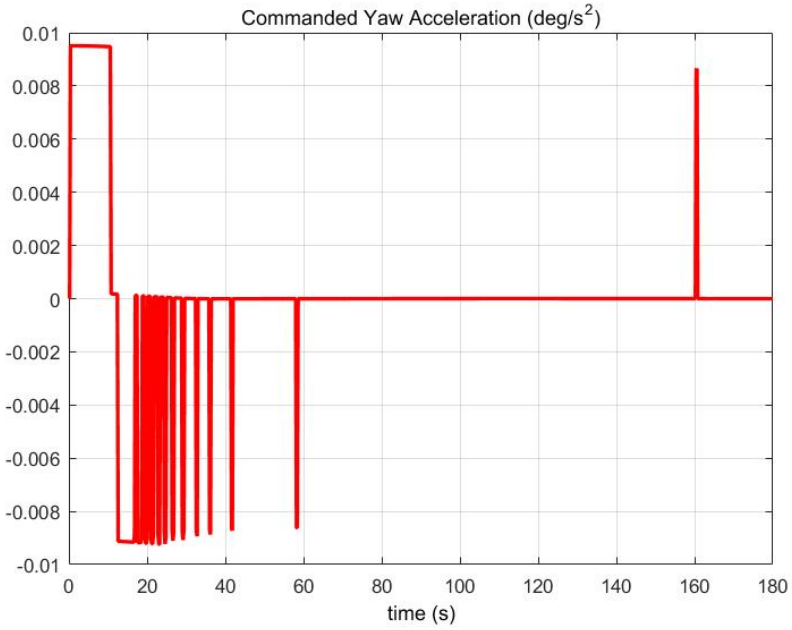

Figure 7.9: The angular acceleration of the satellite's yaw in relation to time. Note that the angular acceleration tries to use the least amount of thrust to reduce fuel consumption. When compared to Figure 7.17 the affects the thrust has on the velocity can be easily seen.

7.2 De-tumbling and Reorientation

This simulation has the satellite start with it both being off its targeted orientation and with an angular velocity. In the previous section, Table 6.7 showed the values of the satellites starting angular position and velocity. This slight angular velocity has a major impact due to the low torque the thrusters were able to produce. End goals for the satellite shown in Table 6.5 can also be seen in the previous chapter.

In Figure 7.10, the angle of the pitch starts at an offset of 1 degree, then maneuvers to 0 degrees after slowing its angular velocity. In Figure 7.11 the satellite is already rotating at a 0.3 degrees per second angular velocity.

In Figure 7.11 is the angular velocity of the pitch in relation to time. When compared with Figure 7.10 there are key points to make note of such as how the satellite first slows its angular velocity before it is able to then correct its position. In Figure 7.12 the commanded acceleration is shown. It is apparent that the acceleration that is commanded is used to slow the angular velocity before ensuring that the satellite starts to move into the desired position. Once it gets close to its desired position it does its best to maintain that position.

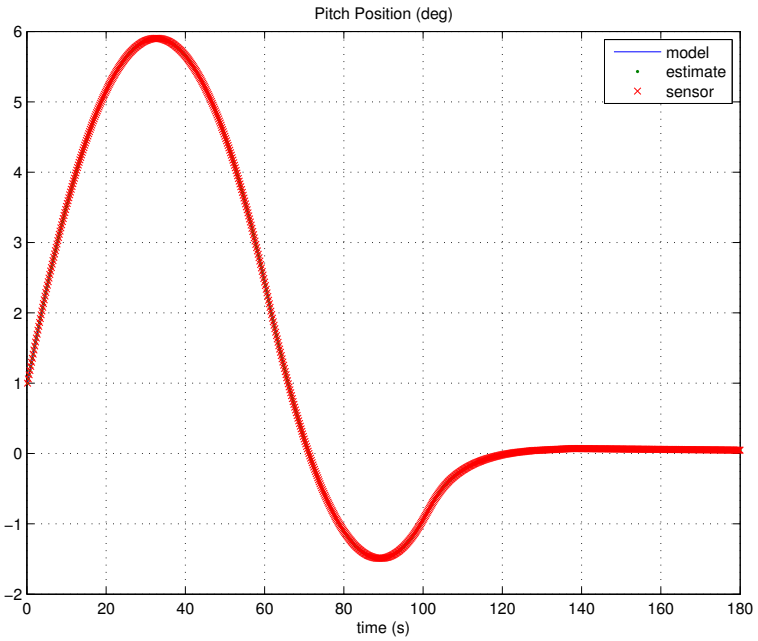

Figure 7.10: The angular position of the satellite's pitch in relation to time. Note that the angle starts at 1 degree and ends at 0 degrees.

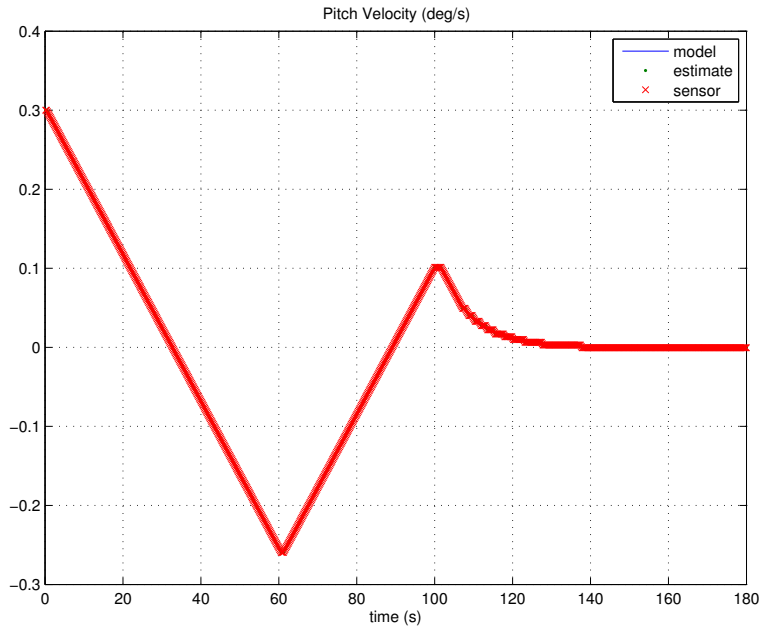

Figure 7.11: The angular velocity of the satellite's pitch in relation to time. Note that the angle starts at 0.3 degrees per second and ends at 0 degrees per second.

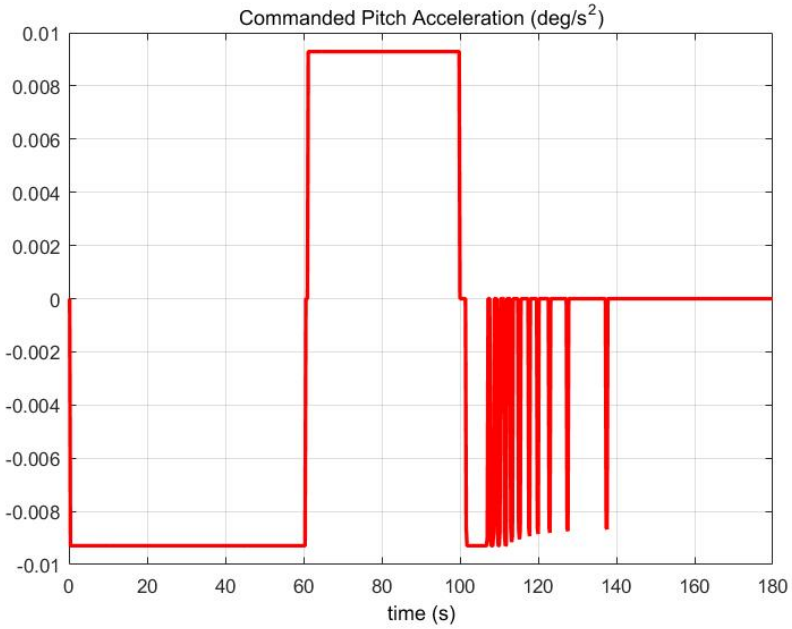

Figure 7.12: The angular velocity of the satellite's pitch in relation to time. Note that the angle starts at 0.3 degrees per second and ends at 0 degrees per second.

The end result is that the thrusters allow the satellite to reach close its desired goal along with maintaining its position in the pitch position. At the same time due to how the controller is keyed to the satellite the thruster usage is kept down. At this point the fine tuning of

the angular position and velocity of the pitch can be adjusted by other attitude controllers such as momentum wheels.

As for the Roll and Yaw which are coupled together the GNC is also able to attain the desired orientation. As seen in Figures 7.13 and 7.16 the satellite is able to reach close to its desired goal. They are within 0.1 degrees of the target point and if given enough time the current angular velocity will eventually allow the satellite to reach its goal.

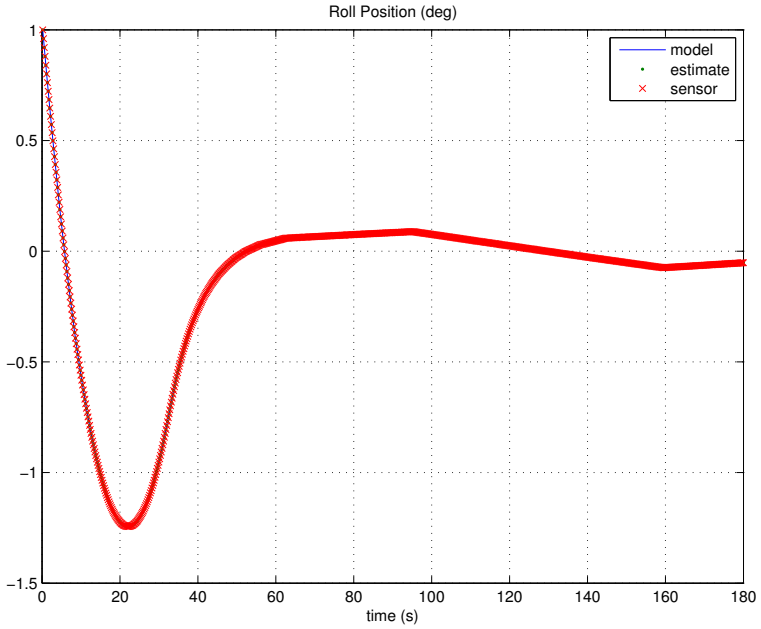

Figure 7.13: The angular position of the satellite's roll in relation to time. Note that the angle starts at 1 degrees and ends close to 0 degrees.

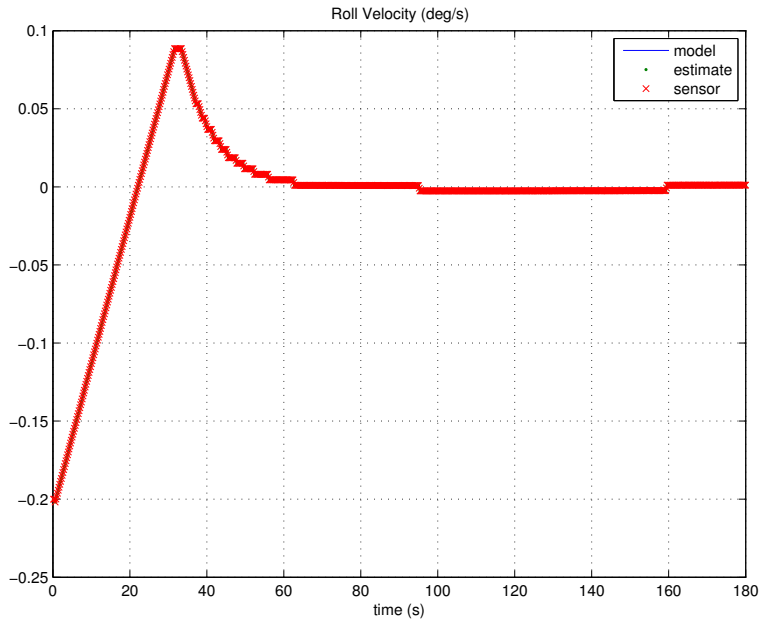

Figure 7.14: The angular velocity of the satellite's roll in relation to time. Note that the angular velocity started at -0.2 degrees per second and ends close to 0 degrees per second.

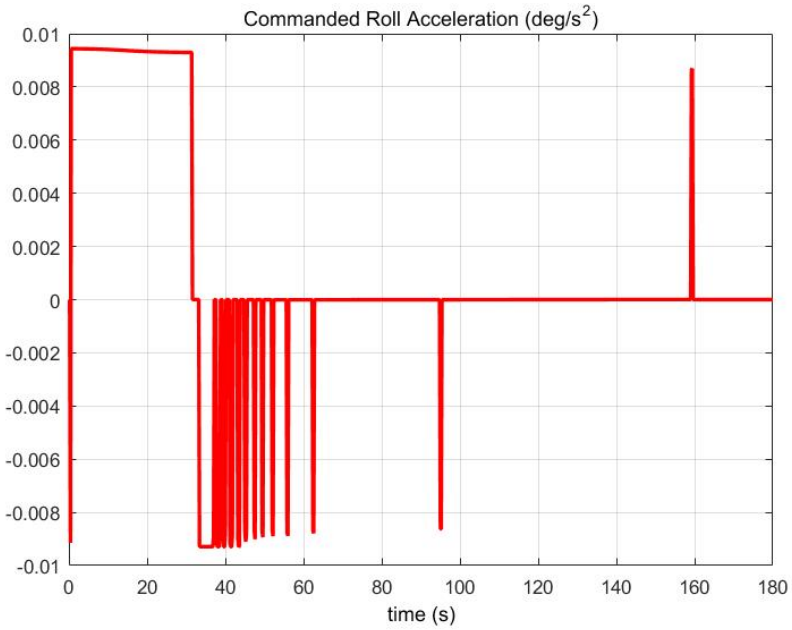

Figure 7.15: The angular acceleration of the satellite's roll in relation to time. Note that the angular acceleration tries to use the least amount of thrust to reduce fuel consumption. When compared to Figure 7.14 the affects the thrust has on the velocity can be easily seen.

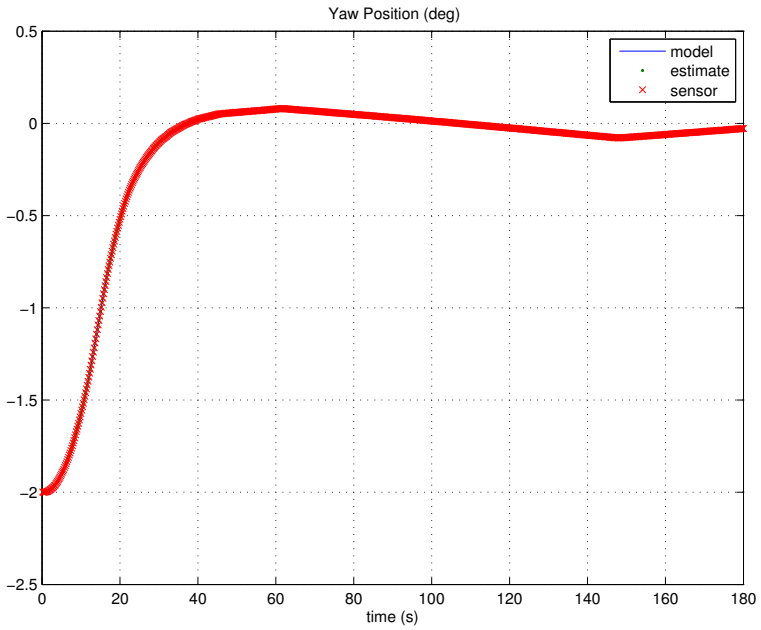

Figure 7.16: The angular position of the satellite's yaw in relation to time. Note that the angle started at -2 degrees and ends at 0 degrees.

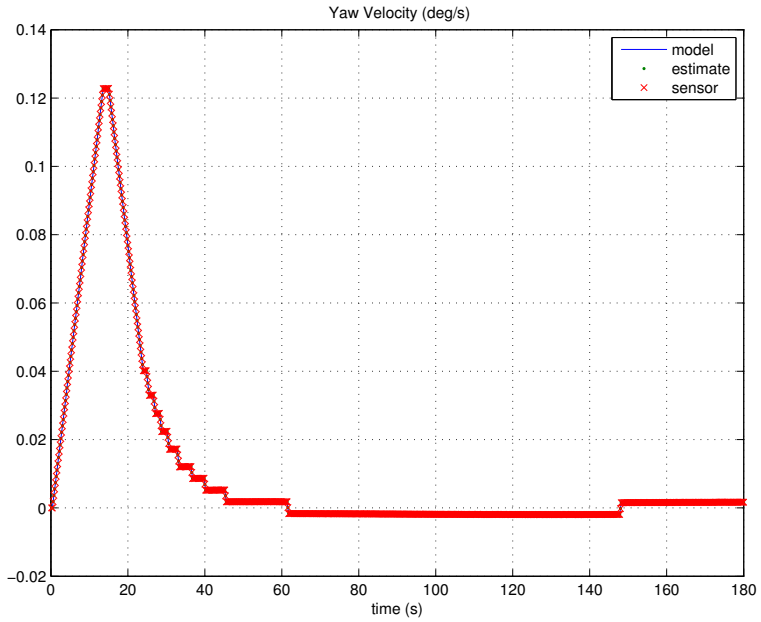

Figure 7.17: The angular velocity of the satellite's yaw in relation to time. Note that the angular velocity started at 0 degrees per second and ends close to 0 degrees per second.

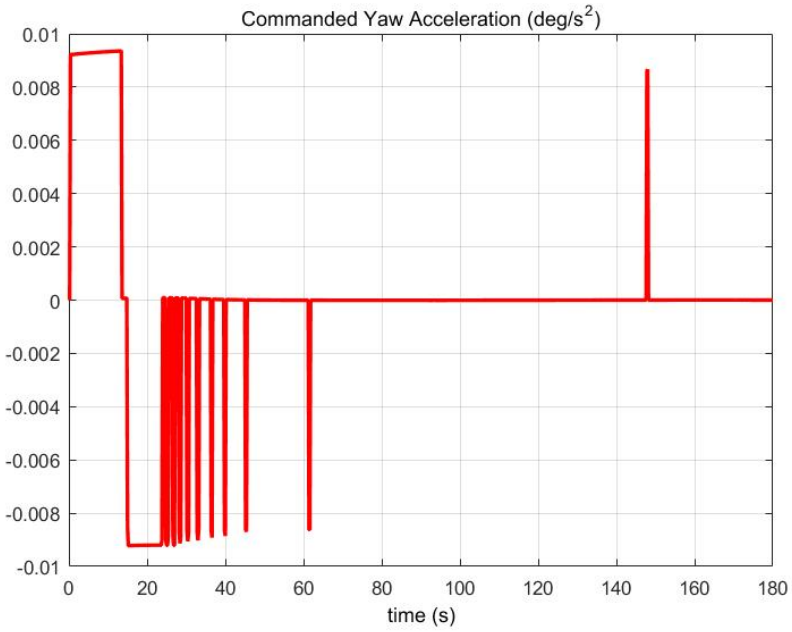

Figure 7.18: The angular acceleration of the satellite's yaw in relation to time. Note that the angular acceleration tries to use the least amount of thrust to reduce fuel consumption. When compared to Figure 7.17 the affects the thrust has on the velocity can be easily seen.

The angular velocity of the satellite for both the roll started at -0.2 degrees per second while the yaw started at rest. Due to how the angular velocity was coupled together the two axis need to take into account each other while doing the simulations. Due to the fact that the thrusters were set to simulate its use as a bang-bang actuator.

In Figures 7.15 and 7.18 the commanded acceleration that acted upon the roll and yaw axis of the satellite are shown. The satellite uses a bang-bang controller for the thrusters to reduce the fuel consumption and to simplify the model.

As with the pitch axis the thrusters usage was kept down after the initial burns. Any additional thruster activation was used primarily to maintain the attitude or adjust the angular velocity as it reached its target point.

In Figures 7.19, 7.20, and 7.21 the covariance of the angular positions are shown. Along with the covariance of the whole simulation, a zoomed in portion of the last 20 seconds is shown. The errors of the estimation of the Extended Kalman filter can be seen to converge for all three cases. Eventually after the initial 100 seconds, the convergence slows to a point where it was no longer noticeable unless zoomed in.

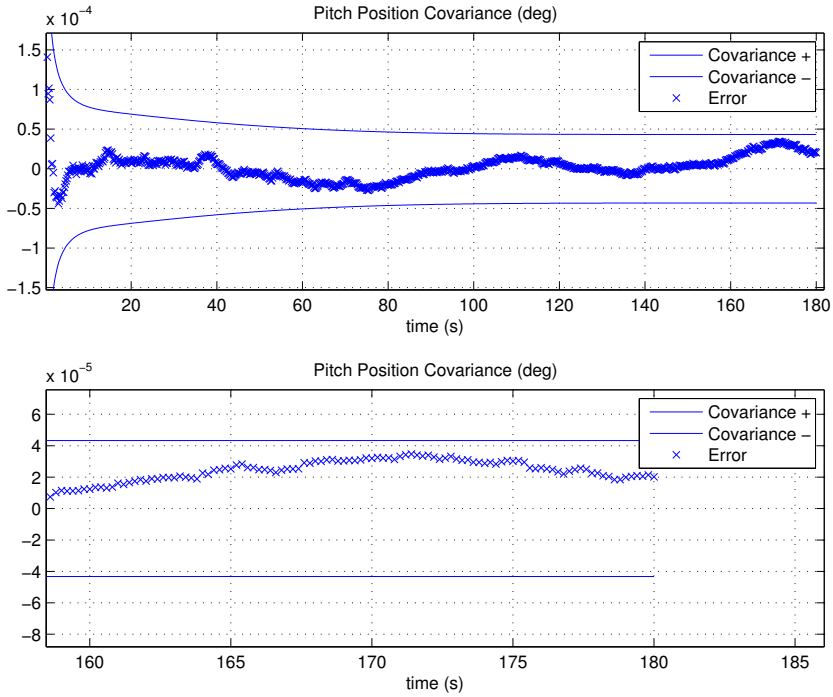

Figure 7.19: The covariance of the pitch angular position. The second subplot shows the last 20 seconds of the simulation.

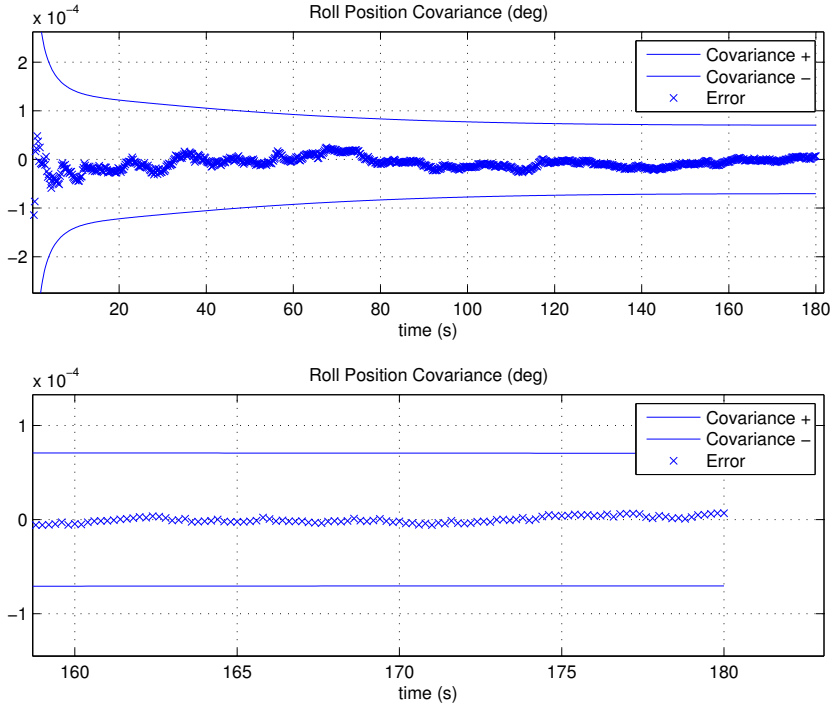

Figure 7.20: The covariance of the roll angular position. The second subplot shows the last 20 seconds of the simulation.

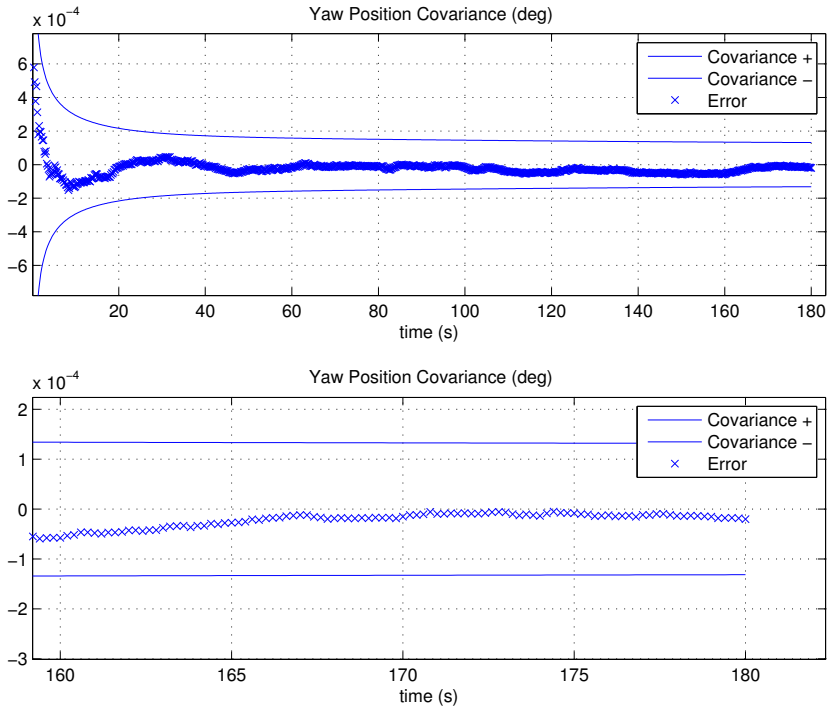

Figure 7.21: The covariance of the yaw angular position. The seoncd subplot shows the lat 20 seconds of the simulation.

Along with Figures 7.22, 7.23, and 7.24 which display the velocity covariance of the system. Again the last 20 seconds of the simulation was zoomed in to show that the errors stayed within the covariance of the Extended Kalman Filter. Though in Figure 7.22 one can see that the errors did come close to exceeding the covariance several times.

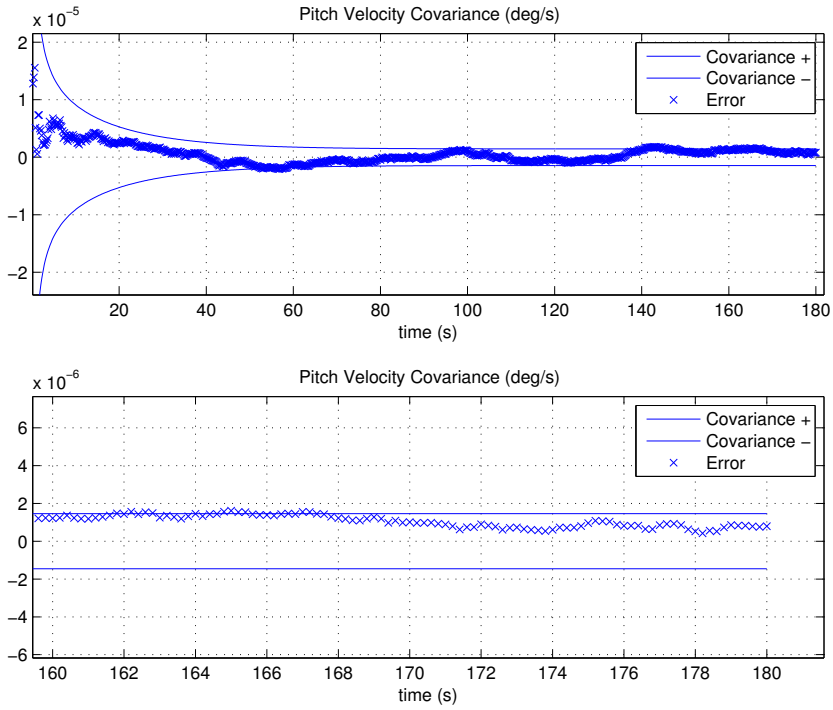

Figure 7.22: The covariance of the pitch angular velocity. The second subplot shows the last 20 seconds of the simulation. The errors do come close to the bounds of the covariance.

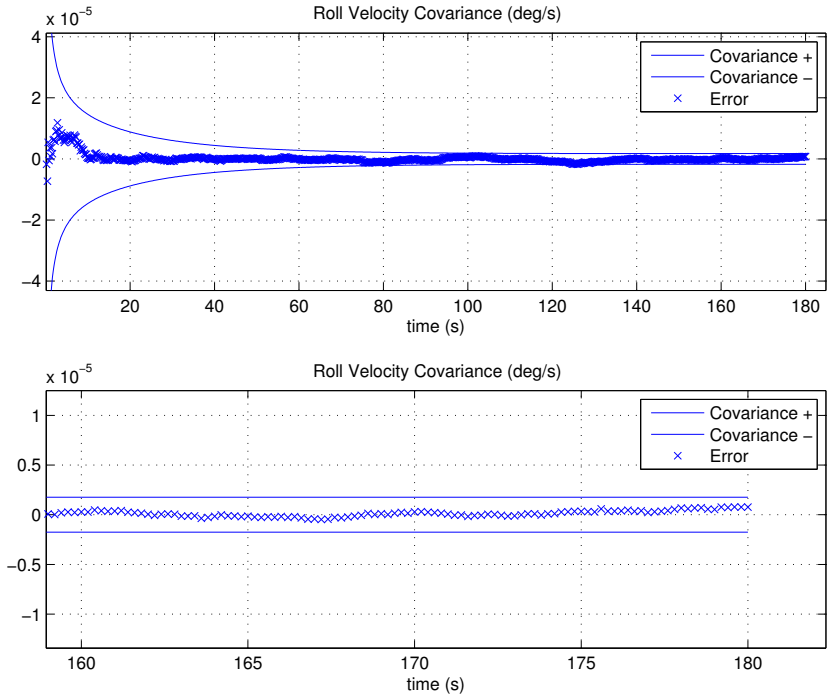

Figure 7.23: The covariance of the roll angular velocity. The second subplot shows the last 20 seconds of the simulation.

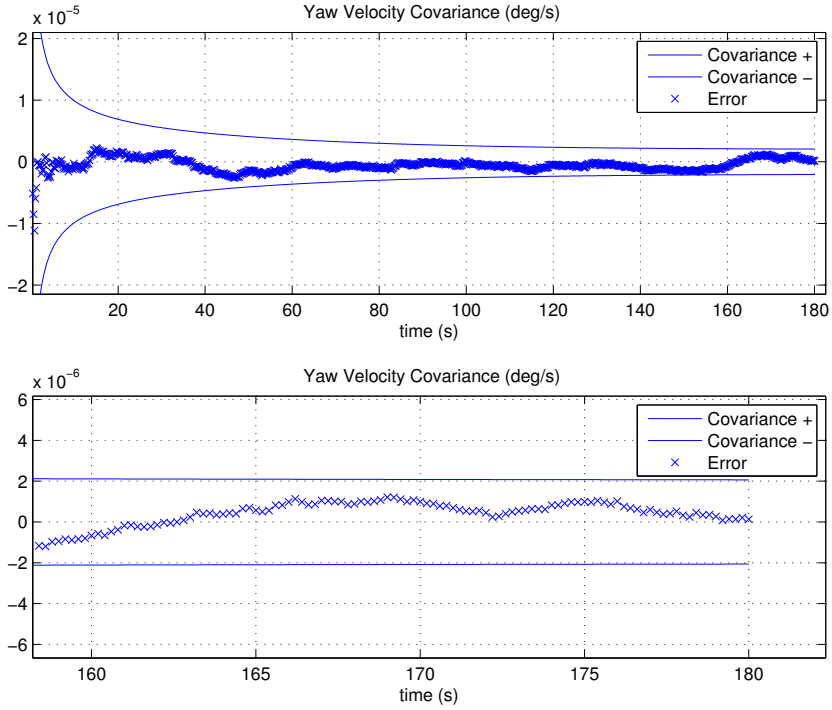

Figure 7.24: The covariance of the yaw angular velocity. The second subplot shows the last 20 seconds of the simulation.

8 ANALYSIS AND COMPARISON

As seen in the previous section the combined GNC system does allow for a satellite to reach its desired orientation. The guidance system helps to create a more stable set of commands which, when combined with the PD controller, help the satellite reach its goal. In many ways the Quartic polynomial law equation and the PD controller have very similar outputs which helps both of them to work off each other in the package.

When comparing the results with a study by Hu Min it was apparent that a closed loop system can be forced into a loop of constant thruster activation [64]. Eventually the simulation showed that the satellite's thrusters were in a loop scenario where it was overshooting its goal and would constantly over compensate. This is a clear example on why the coefficients used for the Guidance and Control portions are key to an efficient and effective controller.

Another example would be a study done for the FalconSat-3[7]. In this study the PD controller was used, similarly to the simulations in the previous section. However for this study a cutoff point for the on off switch for the thrusters was implemented. They called this the dead-zones and also made note that the gains for the P and D are vital for the controller. Too high and the satellite's thrusters would be constantly be activated. Too low and the satellite won't be able to reach its goal in time, or if at all.

Similarly for this series of simulations, the controller had to be constantly tweaked and adjusted. Scaling down to take into account that the thrust output of the system was small. The initial round of simulations did run into problems of thrusters being constantly being activated to over compensate for small errors.

Further studies on the viability of using E-Guidance as opposed to the Quartic would be an interesting comparison. Especially on seeing how it will affect the usage of thrusters and if it can help create a more efficient guidance law.

8.1 Guidance vs Control

The primary purpose of these simulations was to demonstrate the integration of GNC for attitude using Klumpp's Apollo lunar guidance law. As such, the simulations were used a a proof of concept that such an integration would work and as a result used simple maneuvers that did not require a re-targeting procedure. This resulted in the final state being the target state.

It had been noted that due to the simplicity of the problem, the results are show a similarity towards a pure bang-bang controller. This is true for simple orientation maneuvers, however had there been a moving target, the guidance law and target would have made a major difference. Especially when they can help ensure that the satellite is able to properly track its

target. This is due to how the guidance would be able to update the target state, and with these constant updates the satellite would eventually be capable of following the targets path. Even with this, the simulations do demonstrate that the guidance law can and will work for attitude dynamics.

9 CONCLUSION

This paper goes into detail the simulations that have been run for a complete GNC system for a small satellite in a circular orbit. The current simulations show that it is possible for this system to maintain control and orient itself using micro-thrusters in a desired position with minimal input from external sources.

In particular, this study applies polynomial guidance function in conjunction with navigation and control functions to create a closed loop system. While the navigation used is the standard navigation function with an EKF filter with IMU and GPS sensors, the Guidance portion of the GNC system is something that has yet to be fully explored. With the integrated on-board guidance and navigation, the PD controller is capable of achieving its goals in the simulations.

The real-time targeting has been considered for the first time as part of the proposed on-board attitude guidance. The target state included the Euler angles and angular rates. This is the main reason for considering the proposed guidance as the ”target-relative attitude guidance”.

This allows us to create a real time on-board attitude guidance using the polynomial method developed by Klumpp for a translational motion of Apollo landers. However, such a method has shown to be currently limited in its scope. The simulations were conducted for the purposes of de-tumbling and re-orientation. As a result the results from these simulations show that the guidance has a similarity with a bang-bang controller.

Future steps to be taken would be increasing the complexity of the maneuvers to be attempted by the system. As the current GNC system is only considering a simple maneuver and requires more adjustments. This would involve adjusting the guidance methodology and refining the targeting procedures used. At the same time additional satellites can be added into the problem for formation maneuvers. Additionally some disturbances that act upon satellites were not considered in this simulation, thus modifications must be made to take these into account. Furthermore a direct comparison between guidance methods would help in furthering develop an autonomous system.

Bibliography

[1] G. H. Born, "Coordinate systems," feb 2001.

[2] D. A. Vallado, *Fundamentals of Astrodyanamics and Applications*. Microcosm Press, third ed., 2007.

[3] N. Pokrupa and N. Ahlgren, "One year of in-flight results from the prisma formation flying demonstration mission," in *SSC11-III-2*.

[4] S. n Mun oz, "The fastrac mission: Operations summary and preliminary experiment results," in *SSC11-III-4*.

[5] E. Good, *An analysis of Manuver Characteristics and Propulsion System Sizing Parameters For Proximity Maneuvers Performed by A Small Inspector Spacecraft*. PhD thesis, University of Kansas, 2005.

[6] D. Azimov, "D.m. automated, real-time targeting and guidance software for lunar-descent and precision landing. final report," tech. rep., NASA SBIR, 2009.

[7] P. Tisa and P. Vergez, "Performance analysis of control algorithms for falconsat-3," in *16th AAS/AIAA space flight mechanics conference*, 2006.

[8] M. R. Greene, *The attitude determination and control system of the generic nanosatellite bus*. PhD thesis, University of Toronto Institute for Aerospace Studies, 2009.

[9] L. Souza and R. Gonzales, "Application of the state-dependent riccati equation and kalman filter techniques to the design of a satellite control system," *Shock and vibration*, vol. 19, no. 5, pp. 939–946, 2012.

[10] H. Min, Z. Guoqiang, and G. Yudong, "Thruster control for micro-satellite attitude and hardware-in-the-loop demonstration," in *Industrial Control and Electronics Engineering (ICICEE), 2012 International Conference on*, pp. 588–591, IEEE, 2012.

[11] F. G.F., P. J.D., and E.-N. A., *Feedback Control of Dynamic Systems*. Pearson Education, sixth ed., 2010.

[12] C. L. Phillips and J. M. Parr, *Feedback Control Systems*. fifth ed., 2011.

[13] S. Haykin and B. Veen, *Signals and Systems*. John Wiley & Sons, 1999.

[14] G. Thaler, *Automatic Control Systems*. West Publishing Company., 1989.

[15] F. Raven, *Automatic Control Engineering.* McGraw-Hill Book Company, 1987.

[16] W. Brogan, *Modern Control Theory*. Prentice-Hall, Inc, 1982.

[17] H. Ozbay, *Introduction to Feedback Control Theory*. CRC Press, 1999.

[18] N. B.N, *Nonlinear control systems.* 2003.

[19] Ø. Hegrenæs, J. T. Gravdahl, and P. Tøndel, "Spacecraft attitude control using explicit model predictive control," *Automatica*, vol. 41, no. 12, pp. 2107–2114, 2005.

[20] Y. Lv, Q. Hu, G. Ma, and J. Zhang, "Attitude cooperative control of spacecraft formation via output-feedback," *Aircraft Engineering and Aerospace Technology*, vol. 84, no. 5, pp. 321–329, 2012.

[21] I. Mainenti-Lopes, L. Souza, and F. De Sousa, "Design of a nonlinear controller for a rigid-flexible satellite using multi-objective generalized extremal optimization with real codification," *Shock and Vibration*, vol. 19, no. 5, pp. 947–956, 2012.

[22] T.-V. Chelaru, A.-M. Stoica, and A. Chelaru, "Attitude control system design for small satellites using gradient-based methods," in *Recent Advances in Space Technologies (RAST), 2013 6th International Conference on*, pp. 505–510, IEEE, 2013.

[23] M. D. Shuster, "A survey of attitude representations," *Navigation*, vol. 8, no. 9, pp. 439–517, 1993.

[24] M. Lee, *Active control of the attitude motion and structural vibration of a flexible satellite by jet thrusters*. 2006.

[25] M. Mihailovic, T. Mathew, J. Creemer, B. Zandbergen, and P. Sarro, "Mems silicon-based resistojet micro-thruster for attitude control of nano-satellites," in *Solid-State Sensors, Actuators and Microsystems Conference (TRANSDUCERS), 2011 16th International*, pp. 262–265, IEEE, 2011.

[26] F. Mingireanu and M. Stoia-Djeska, "Small hybrid thruster development for small satellite attitude control system," in *Recent Advances in Space Technologies (RAST), 2013 6th International Conference on*, pp. 297–301, IEEE, 2013.

[27] S. Marcuccio, S. Giannelli, and M. Andrenucci, "Attitude and orbit control of small satellites and constellations with feep thrusters," *Electric Rocket Propulsion Society*, 1997.

[28] M. D. Van de Loo, *CubeSat attitude control using micronewton electrospray thruster actuation*. PhD thesis, Massachusetts Institute of Technology, 2014.

[29] F. Rysanek, J. Hartmann, J. Schein, and R. Binder, "Microvacuum arc thruster design for a cubesat class satellite," 2002.

[30] N. A. Chaturvedi, A. K. Sanyal, and N. H. McClamroch, "Rigid-body attitude control," *Control Systems, IEEE*, vol. 31, no. 3, pp. 30–51, 2011.

[31] R. Kristiansen, P. Nicklasson, and J. Gravdahl, "Satellite attitude control by quaternion-based backstepping," *Control Systems Technology, IEEE Transactions on*, vol. 17, pp. 227–232, Jan 2009.

[32] M. H. Kaplan, "Modern spacecraft dynamics and control," *New York, John Wiley and Sons, Inc., 1976. 427 p.*, vol. 1, 1976.

[33] J. Koenig, "A novel attitude guidance algorithm for exclusion zone avoidance," in *Aerospace conference, 2009 IEEE*, pp. 1–10, March 2009.

[34] K. L. Makovec, *A nonlinear magnetic controller for three-axis stability of nanosatellites*. PhD thesis, Virginia Polytechnic Institute and State University, 2001.

[35] W. Fehse, *Automated rendezvous and docking of spacecraft*, vol. 16. Cambridge university press, 2003.

[36] G. Cherry, "E-guidance - a general explicit, optimizing guidance law for rocket propelled spacecraft," tech. rep., MIT Instrumentation Laboratory, 1964.

[37] A. R. Klumpp, "Apollo lunar-descent guidance. apollo guidance navigation control," tech. rep., MIT, Cambridge, 1971.

[38] H. J. Kelley, "Guidance theory and extremal fields," *IEEE Transactions on Automatic Control*, 1962.

[39] D. M. Azimov and R. H. Bishop, "Optimal trajectories for space guidance. new trends in astrodynamics and applications," *Annals of the New York Academy of Sciences*, vol. 1065, no. 189-209, 2005.

[40] C. Lin, *Modern Navigation, Guidance and Control Processing.* Prentice Hall, Englewood Cliffs, New Jersey,, 1991.

[41] G. Ducard, *Fault-tolerant Flight Control and Guidance Systems*. Springer-Verlag. New York., 2009.

[42] T. Yang, "A targeting scheme for fuel optimal rocket trajectories with applications to the lm descent braking phase," technical memorandum, Bellcomm, 1971.

[43] B. I. D. Systems, "Orbital express demonstration system overview," tech. rep., The Boeing Company, 2010.

[44] D. Azimov, "Summary of some small satellite missions of interest," 2012.

[45] P. Z. Schulte, "Prox-1 guidance, navigation, & control overview: Development, algorithms, and integrated simulation," 2014.

[46] N. H. Roth, *Navigation and control design for the CanX-4/-5 satellite formation flying mission*. PhD thesis, 2011.

[47] D. D. Bhanderi, *Spacecraft Attitude Determination with Earth Albedo Corretted Sun Sensor Measurements*. Department of Control Engineering, Aalborg university, 2005.

[48] D. Azimov, "Me 696 gnc." University Course, jan 2013.

[49] J. L. Junkins, *How Nonlinear is It? A Tutorial on Judicious Coordinates for Orbit and Attitude Dyanamics*. AAS Publications Office, 2003.

[50] F. Martel, L. Perna, and P. Lozano, "Miniature ion electrospray thrusters and performance test on cubesats," 2012.

[51] D. Azimov, "State estimation and filtering techniques." University of Hawaii at Manoa, feb 2012.

[52] A. Valdes and K. Khorasani, "Dynamic neural network-based pulsed plasma thruster (ppt) fault detection and isolation for the attitude control system of a satellite," in *Neural Networks, 2008. IJCNN 2008.(IEEE World Congress on Computational Intelligence). IEEE International Joint Conference on*, pp. 2689–2695, IEEE, 2008.

[53] D. T. Schmuland, "Hydrazine propulsion module for cubesats," tech. rep., SSC11-X-4.

[54] W. N. S. et al, "Electrically controlled extinguishable solid propellants* solid state digital propulsion -cluster thrusters- for small satellites, using high performance," tech. rep., SSC05-XI-3.

[55] S. Mauthe, "The design and test of a compact propulsion system for canx nanosatellite formation flying," tech. rep., SSC05-VI-5.

[56] D. Spence., "A compact low-power high-isp thruster for microsatellites," tech. rep., SSC08-VII-4.

[57] D. Hinkley, "A novel cold gas propulsion system for nanosatellites and picosatellites.," tech. rep.

[58] R. Pahl, "Design, test, and validation of a refrigerant-based cold-gas propulsion system for small satellite," tech. rep.

[59] M. Tsay, "Micro rf ion engine for small satellite applications," tech. rep., SSC09-II-1.

[60] M. Persson, "The first in-space demonstration of a green propulsion system," tech. rep., SSC10-XI-2.

[61] C. Clark, "An off-the-shelf electric propulsion system for cubesats," tech. rep., SSC11-VI-12.

[62] A. Klumpp, "Manually retargeted automatic landing system for the lunar module (lm).," *Journal of Spacecraft and Rockets*, feb 1968.

[63] A. Klumpp, "Apollo lunar descent guidance.," *Automatica*, vol. 10, pp. 133–146, 1974.

[64] H. Min, Z. Guoqiang, and G. Yudong, "Thruster control for micro-satellite attitude and hardware-in-the-loop demonstration," in *Industrial Control and Electronics Engineering (ICICEE), 2012 International Conference on*, pp. 588–591, IEEE, 2012.

[65] J. L. Smith, "Attitude determination and control suitable for micro-spacecraft," in *Aerospace Conference Proceedings, 2000 IEEE*, vol. 7, pp. 143–165, IEEE, 2000.

[66] F. Miranda, "Magnetic attitude stabilization of satellites using guidance control," in *ICNAAM 2010: International Conference of Numerical Analysis and Applied Mathematics 2010*, vol. 1281, pp. 477–480, AIP Publishing, 2010.

[67] R. Kristiansen and P. J. Nicklasson, "Satellite attitude control by quaternion-based backstepping," in *American Control Conference, 2005. Proceedings of the 2005*, pp. 907–912, IEEE, 2005.

[68] C.-F. Lin, *Modern navigation, guidance, and control processing*, vol. 2. Prentice Hall Englewood Cliffs, New Jersey, 1991.

[69] F. B. Zazzera, "Spacecraft attitude dynamics and control." University Lecture.

[70] NASA, "Project Apollo Coordinate System Standards," tech. rep., NASA, 1965.

[71] P. G. Savage, "Strapdown inertial navigation integration algorithm design part 1: Attitude algorithms," *Journal of guidance, control, and dynamics*, vol. 21, no. 1, pp. 19–28, 1998.

[72] P. G. Savage, "Strapdown inertial navigation integration algorithm design part 2: Velocity and position algorithms," *Journal of Guidance, Control, and Dynamics*, vol. 21, no. 2, pp. 208–221, 1998.

[73] E. Muller and P. Kachmar, "The apollo rendezvous navigation filter theory, description and performance," tech. rep., Masschusetts Institue of Technology, 1970.

[74] F. L. M. Y. C. John L. Crassidis, "Survey of nonlinear attitude estimation methods," *Journal of Guidance, Control, and Dynamics*, vol. 30, no. 1, pp. 12–28, 2007.

[75] M. Wiegand, "Autonomous satellite navigation via kalman filtering of magnetometer data," *Acto Astronautica*, vol. 38, no. 4-8, pp. 395–403, 1996.

[76] D. W. S. V. J. Lappas and D. C. I. Underwood, "Attitude control for small satellites using control moment gyros," *AcraA srmnautic*, vol. 51, no. 1-9, pp. 101–111, 2002.

[77] P. Appel, "Attitude estimation from magnetometer and earth-albedo-corrected coarse sun sensor measurements," *Acta Astronautica*, vol. 56, pp. 115–126.

[78] J. C. Springmann, A. J. Sloboda, A. T. Klesh, M. W. Bennett, and J. W.Cutler, "The attitude determination system of the rax satellite," *Acta Astronautica*, vol. 75, pp. 120–135, 2012.

[79] G. Guglieri, F. Maroglio, P. Pellegrino, and L. Torre, "Design and development of guidance navigation and control algorithms for spacecraft rendezvous and docking experimentation," *Acta Astronautica*, vol. 94, pp. 395–408, 2014.

[80] C. Z. Shaobo Ni, "Attitude determination of nano satellite based on gyroscope, sunseonr, and magnetometer," *Procedia Engineering*, no. 15, pp. 959–963, 2011.

[81] J. L. Crassidis and F. L. Markley, "Unscented filtering for spacecraft attitude estimation," *Journal of guidance, control, and dynamics*, vol. 26, no. 4, pp. 536–542, 2003.

[82] T.-V. Chelaru, C. Barbu, and A. Chelaru, "Mathematical model for small satellites, using attitude and rotation angles,"

[83] M. A. Nunes, T. C. Sorensen, and E. J. Pilger, "On the development of a 6 dof gnc framework for docking multiple small satellites,"

[84] M. A. Nunes, T. C. Sorensen, and E. J. Pilger, "Cooperative control of multiple small satellites using the comprehensive open-architecture space mission operations system (cosmos),"

[85] M. Grewal and M. Shiva, "Application of kalman filtering to gyroless attitude determination and control system for environmental satellites," in *Decision and Control, 1995., Proceedings of the 34th IEEE Conference on*, vol. 2, pp. 1544–1552, IEEE, 1995.

[86] G. Arantes and L. S. Martins-Filho, "Guidance and control of position and attitude for rendezvous and dock/berthing with a noncooperative/target spacecraft," *Mathematical Problems in Engineering*, vol. 2014, 2014.

[87] P. Guan, X. Liu, and X. Liu, "Adaptive fuzzy control for satellite," in *Intelligent Control and Automation, 2006. WCICA 2006. The Sixth World Congress on*, vol. 1, pp. 124–128, IEEE, 2006.

[88] F. Zhao, P. Cui, R. Xu, and Z. Li, "Attitude navigation for deep space explorer based on mission planning," in *Control and Decision Conference (2014 CCDC), The 26th Chinese*, pp. 2088–2093, IEEE, 2014.

[89] J. Rao, H. Qiu, and K. Xiong, "Analysis of the factors influencing the attitude determination accuracy based on orthogonal experiment," in *Guidance, Navigation and Control Conference (CGNCC), 2014 IEEE Chinese*, pp. 1385–1389, IEEE, 2014.

[90] M. L. McGuire and R. M. Myers, *Pulsed plasma thrusters for small spacecraft attitude control*. National Aeronautics and Space Administration, 1996.

[91] H. Kjellberg and E. G. Lightsey, "A constrained attitude control module for small satellites," 2012.

[92] K. L. Makovec, A. J. Turner, and C. D. Hall, "Design and implementation of a nanosatellite attitude determination and control system," in *Proceedings of the 2001 AAS/AIAA Astrodynamics Specialists Conference, Quebec City, Quebec*, no. 0.5, p. 1, 2001.

[93] Y. Kusuda and M. Takahashi, "Feedback control with nominal inputs for agile satellites using control moment gyros," *Journal of Guidance, Control, and Dynamics*, vol. 34, no. 4, pp. 1209–1218, 2011.

[94] W. H. Steyn, Y. Hashida, and V. Lappas, "An attitude control system and commissioning results of the snap-1 nanosatellite," 2000.

[95] T.-V. Chelaru, A.-M. Stoica, and A. Chelaru, "Attitude control synthesis for small satellites using gradient method part i nonlinear equations," *INCAS Bulletin, ISSN*, pp. 2066–8201.

[96] T.-V. Chelaru, A.-M. Stoica, and A. Chelaru, "Attitude control synthesis for small satellites using gradient method part ii linear equations, synthesis," *INCAS Bulletin*, vol. 5, no. 1, 2013.

[97] A. Zanchettin and M. Lovera, "H attitude control of magnetically actuated satellites," in *IFAC World Congress*, vol. 18, pp. 8479–8484, 2011.

[98] M. Fournier, *Attitude Determination and Control Hardware Development for Small Satellites*. PhD thesis, 2011.

[99] M. T. Nehrenz, "Initial design and simulation of the attitude determination and control system for lightsail-1," 2010.

[100] J. Smith, C. Wood, K. Reister, D. Forrest, K. Levenson, W. Vestrand, C. Whitford, D. Watson, and A. Owens, "Low-cost attitude determination and control for small satellites," 1996.

[101] H. Fisher, T. Strikwerda, C. Kilgus, L. Frank, and M. Shuster, "Autonomous, all-stellar attitude determination experiment: ground test results," in *Proceedings of the Rocky Mountain Guidance and Control Conference, Paper AAS*, pp. 91–025, 1991.

[102] W. Ren, T. Zhang, Z. Huang, J. Liang, J. Gong, and B. Liu, "Real-time simulation system of satellite attitude reconfigurable control based on vxworks," in *Guidance, Navigation and Control Conference (CGNCC), 2014 IEEE Chinese*, pp. 2577–2580, IEEE, 2014.

[103] W. H. Steyn, *A multi-mode attitude determination and control system for small satellites*. PhD thesis, Stellenbosch: Stellenbosch University, 1995.

[104] J. Z. J. Mueller, R. Hofer, "Survey of propulsion technologies applicable to cubesats," tech. rep., Jet Propulsion Laboratory, NASA, 2010.

[105] T. Sorensen, "Development of a comprehensive mission operations system designed to operate multiple small satellites," 25th Annual AIAA/USU Conference on Small Satellites, 2011.

[106] Tretyakov, V.I., and et al., "The first stage of the btn neutron space experiment on board the russian segment of the international space station," *Cosmic Research*, vol. 48, no. 4, pp. 285–299, 2010.

[107] D. Hull, "Optimal guidance for quasi-planar lunar ascent," *Journal of Optimization Theory and Applications*, vol. 151, pp. 353–372, nov 2011.

[108] C. Epp and T. Smith, "The autonomous precision landing and hazard detection and avoidance technology (alhat). go for lunar landing: From terminal descent to touchdown," p. 7, mar 2008.

[109] A. D.M. and B. R.H., "Reconstruction of apollo targeting and guidance for powered lunar descent. new trends in astrodynamics and applications v," 2008.

[110] D. Burkhart, T. Crain, R. H. Bishop, D. M. Azimov, C. Chomel, L. Croix, and M. Heyne, "MSL: EDL GNC. peer review EDL navigation.," tech. rep., Jet Propulsion Laboratory, 2004.

[111] A. J. H. M. L. J. Ogilvie, A., "Autonomous satellite servicing using the orbital express demonstration manipulator system.," in *Proceedings of the 9th International Symposium on Artificial Intelligence, Robotics and Automation in Space.*, p. 8, feb 2008.

[112] Z. Y. . Yang Lin, Gaofei Zhang, "A novel design of mems based solid propellant micro propulsion array for micro satellites," tech. rep., SSC05-VIII-4.